ADVANCED AERODYNAMICS AND MULTIPHYSICS

CFD e-Learning

Euler equations and discretization of convection

G. Puigt and H. Deniau

Release 1.1
January 2011

Centre Européen de Recherche et de Formation Avancée en Calcul Scientifique
42 avenue Coriolis – 31057 Toulouse Cedex 1 – France
Tél : +33 5 61 19 31 31 – Fax : +33 5 61 19 30 00
http://www.cerfacs.fr – e-mail: secretar@cerfacs.fr

Contents

Chapter 1

Introduction

This document follows the one on CFD basic concepts[1]. In particular, none of the notations will be recalled. The Navier Stokes equations are written in the following conservative form:

$$\left\{\begin{array}{lcl} \partial_t\rho + \nabla.(\rho\vec{u}) & = & 0 \\ \partial_t(\rho\vec{u}) + \nabla.(\rho\vec{u}\otimes\vec{u}) + \nabla p - \nabla.\tau & = & 0 \\ \partial_t(\rho E) + \nabla.\Big(\vec{u}(\rho E + p)\Big) & = & \nabla.\left(\vec{u}\tau + \lambda\nabla T\right) \end{array}\right. \tag{1.1}$$

where $\tau = \mu(\nabla\vec{u} + \nabla\vec{u}^T) - \dfrac{2\mu}{3}\mathbf{I}\nabla.\vec{u}$ and $\lambda = \dfrac{C_p\mu}{Pr}$.

Under physical assumptions, the Navier Stokes equations are established with an integral formulation and this integral formulation is the basis of the finite volume approach which is chosen for the numerical discretization. Without any loss of generality, let Ω be the space on which the Navier Stokes equations are integrated; one obtains from Eq. 1.1:

$$\left\{\begin{array}{lcl} \dfrac{\partial}{\partial_t}\left(\displaystyle\int_\Omega \rho d\omega\right) + \int_{\partial\Omega}\rho\vec{u}.\vec{n}ds & = & 0 \\ \dfrac{\partial}{\partial_t}\left(\displaystyle\int_\Omega \rho\vec{u} d\omega\right) + \int_{\partial\Omega}\rho(\vec{u}\otimes\vec{u} + p\mathbf{I})\vec{n}ds & = & \displaystyle\int_{\partial\Omega}\tau\vec{n}ds \\ \dfrac{\partial}{\partial_t}\left(\displaystyle\int_\Omega \rho E d\omega\right) + \int_{\partial\Omega}\Big((\rho E + p)\vec{u}.\vec{n}ds\Big) & = & \displaystyle\int_{\partial\Omega}\left(\vec{u}\tau.\vec{n} + \lambda\nabla T.\vec{n}\right)ds \end{array}\right. \tag{1.2}$$

Eq. 1.2 is decomposed in three terms:

- The right hand sides are devoted to diffusion fluxes at mesh interface.
- The left hand sides of the equation are devoted to convection and time terms.

In practice, in a CFD code, one uses one scheme for the convection term, another one for the diffusion flux and finally a third one for the time step. The equations with a null diffusion term are called the Euler's equations. They are obtained formally by taking a null viscosity

[1] *CFD e-Learning, Mesh and discretization*, G. Puigt and H. Deniau, 2010, Edition 1.0

$\mu = 0$ or equivalently an infinite Reynolds number. They are written:

$$\left\{\begin{array}{lcl} \dfrac{\partial}{\partial_t}\left(\displaystyle\int_\Omega \rho d\omega\right) + \displaystyle\int_{\partial\Omega} \rho\vec{u}.\vec{n}ds & = & 0 \\ \dfrac{\partial}{\partial_t}\left(\displaystyle\int_\Omega \rho\vec{u} d\omega\right) + \displaystyle\int_{\partial\Omega} \rho(\vec{u}\otimes\vec{u} + p\mathbf{I})\vec{n}ds & = & 0 \\ \dfrac{\partial}{\partial_t}\left(\displaystyle\int_\Omega \rho E d\omega\right) + \displaystyle\int_{\partial\Omega} \left((\rho E + p)\vec{u}.\vec{n}ds\right) & = & 0. \end{array}\right. \tag{1.3}$$

The Euler's equations are the model problem for the establishment and the analysis of numerical schemes devoted to convection flux integrals. The analysis of the Euler equations will be the basis of the current document.

Chapter 2

Analysis of Euler equations

2.1 Introduction and some reminders on numerical schemes

Proposal, test and validation of numerical schemes are possible through a formalism proposed by mathematicians. This formalism has been presented in another CFD course on the e-learning web page. In this document, our attention is focused on the treatment of the convection flux at the interface between two finite volumes.

2.1.1 Consistence

Theorem 2.1.1. *A numerical scheme is said consistent if the truncation error between the discretized and continuous equations tends to zero when the spatial steps δx, δy, δz and the temporal one δt tend to 0.* In other words, a scheme is said consistent if the discretized equations tend to the continuous ones when the spatial and temporal discretization steps tend to zero.

2.1.2 Stability

Theorem 2.1.2. *Let u_d^n (d meaning discrete) be a discrete solution at time $n\delta t$ for an exact solution u_e. The temporal evolution problem is said stable if the error ε^n at time $n\delta t$ defined by $\varepsilon^n = u_d^n - u_e$ is uniformly limited:*

$$\lim_{n\to\infty} |\varepsilon^n| \leq K \quad \forall t = n\delta t.$$

In other words, a numerical scheme must not increase perturbations during the time steps.

In practice, stability is analyzed by introducing harmonics like $\hat{u}\exp(i(kx - \omega t))$ in the scheme expression; to have convergence of the computation, the amplification factor must be lower than 1.

2.1.3 Convergence

Theorem 2.1.3. *A numerical scheme is convergent if the numerical solution tends to the exact solution when both time and space steps tens to zero.:*

$$\lim_{n\to\infty} |\varepsilon^n| = 0 \text{ quand } \Delta x,\ \Delta y,\ \Delta z,\ \Delta t \text{ tend to } 0 \text{ at } t,\ x,\ y,\ z \text{ fixed.}$$

Remark 2.1.4. *The main difference between convergence and consistence is the application of the method to a solution or not. Therefore, both formalisms are not equivalent!*

2.1.4 Lax theorem

Theorem 2.1.5 (Lax's Theorem)**.** *For a well-posed linear problem (with a unique solution which depends continuously of input data) with boundary conditions and a consistent discretization, stability is a necessary and sufficient condition for convergence.*
This means that:

$$\text{Stability} + \text{Consistence} \Longrightarrow \text{Convergence}$$

2.1.5 Other considerations

Even if the mathematical formalism is quite clear, a consistent and stable numerical scheme only induces no-crash during the iterations process and does not guarantee that the numerical solution will efficiently represent the physical solution. The guarantee of convergence to the "good solution" needs the complementary notions of dissipation and dispersion for a numerical scheme.

Remark 2.1.6. *Dissipation and dispersion will not be addressed in this document.*

2.2 Hyperbolic aspect of the Euler's equations

2.2.1 Preliminary comments

The principle of the finite volume technique is to define an averaged solution over each control volume. As a consequence, the discrete solution is discontinuous at each mesh interface, even if the exact solution is continuous. The only theoretical case for which a solution is continuous is the constant solution. During simulations, due to round off of real representation on computers, the numerical approximation can lead to small variations of the conservative quantities and finally, the "converged" solution is roughly continuous and in practice piecewise constant. The principle of the finite volume approach is therefore to approximate a solution by a piecewise constant solution over each elementary volume. This is the most important point to tackle about the convection schemes and this point will be addressed in the following sections.

2.2.2 Hyperbolic system of equations

Remark 2.2.1. *In the following, we will prove that the Euler's equations are hyperbolic: the Jacobian matrix $A = \partial F/\partial U$ is invertible with real eigenvalues and eigenvectors. The hyperbolic aspect of the equations has a strong consequence: a perturbation at time t will only influence the flow at time $t' > t$. Mathematically, the hyperbolic status plays an important role: it justifies that the converged solution can become discontinuous, even for a smooth initial solution. Taking into account the discontinuity will be addressed by the Rankine Hugoniot's relations which characterize the jumps of the solution. Rankine Hugoniot relations will finally be the key point in the definition of numerical schemes.*

Let us consider the one-dimension Euler's equations written for a perfect gas in a compact form:

$$\frac{\partial U}{\partial t} + \frac{\partial F(U)}{\partial x} = 0, \tag{2.1}$$

with $U = (\rho, \rho u, \rho E)^T$ and $F(U) = (\rho u, \rho u^2 + p, \rho u H)^T$ where $E = e + u^2/2$ is the specific total energy, $H = E + p/\rho$ is the specific total enthalpy, e is the specific internal energy (linked with the temperature $e = C_v T$ with C_v heat capacity at constant volume) and $p = \rho RT = (\gamma - 1)\rho e = \rho R e / C_v$ is the pressure. Eq. 2.1 is the conservative form of Euler's equations and U is called conservative variable. In this section, we assume that the flux F can be differentiated.

Theorem 2.2.2. *Let $A = \partial F / \partial U$ be the Jacobian matrix of the F with respect to the conservative variables which define U:*

$$A = \begin{bmatrix} 0 & 1 & 0 \\ \dfrac{\gamma - 3}{2} u^2 & (3 - \gamma) u & \gamma - 1 \\ u\left((\gamma - 1) u^2 - \gamma E \right) & \gamma E - \dfrac{3}{2} (\gamma - 1) u^2 & \gamma u \end{bmatrix}. \tag{2.2}$$

Proof. The first line of the matrix is easily obtained, considering ρ, ρu and ρE as independent variables. The question concerns therefore the last two lines of A. The solution consists in an expression of p as a function of ρ, ρu and ρE. One knows that:

$$p = \rho RT = \rho \frac{R}{C_v} e = (\gamma - 1)\rho e = (\gamma - 1) \left(\rho E - \frac{(\rho u)^2}{2\rho} \right) \tag{2.3}$$

Let us consider the derivation of $\rho u^2 + p$. Due to Eq. 2.3, we have:

$$\begin{cases} \dfrac{\partial(\rho u^2 + p)}{\partial \rho} &= \dfrac{\partial((\rho u)^2/\rho)}{\partial \rho} + \dfrac{\partial p}{\partial \rho} = -\dfrac{(\rho u)^2}{\rho^2} + \dfrac{\gamma - 1}{2} \dfrac{(\rho u)^2}{\rho^2} = \dfrac{\gamma - 3}{2} u^2 \\ \dfrac{\partial(\rho u^2 + p)}{\partial(\rho u)} &= \dfrac{\partial((\rho u)^2/\rho)}{\partial(\rho u)} + \dfrac{\partial p}{\partial \rho} = 2u - (\gamma - 1)u = (3 - \gamma)u \\ \dfrac{\partial(\rho H)}{\partial(\rho E)} &= \dfrac{\partial((\rho u)^2/\rho)}{\partial(\rho E)} + (\gamma - 1)\dfrac{\partial(\rho E)}{\partial(\rho E)} = \gamma - 1 \end{cases} \tag{2.4}$$

The last line of Eq. 2.2 is obtained following the same kind of relations. This exercise is let to the reader.

□

Using derivation rules, the linearized version of Eq. 2.1 is written:

$$\frac{\partial U}{\partial t} + A \frac{\partial U}{\partial x} = 0. \tag{2.5}$$

Definition 2.2.3. *The system Eq. 2.1 is said* **strongly ill-posed** *if and only if the linearized problem Eq. 2.5 has almost one complex eigenvalue: there exist an eigenvalue λ such that $\lambda \in \mathbb{C}$ and $\lambda \notin \mathbb{R}$.*

Definition 2.2.4. *The linearized system Eq. 2.5 is said* **well-posed** *if and only of if all its eigenvalues are purely real.*

Definition 2.2.5. *The linearized system Eq. 2.5 is said* **weakly well-posed** *if and only of if:*

- *it is well-posed and,*
- *the space based on the eigenvectors is incomplete: there are n eigenvalues and $p < n$ different eigenvectors V_k such that $span(V_1, ..., V_p) \neq \mathbb{R}^n$.*

Definition 2.2.6. *The linearized system Eq. 2.5 with p equations is said* **hyperbolic** *or* **strongly well-posed** *if and only if if it is well-posed and there are p different eigenvalues and therefore p independent eigenvectors.*

Definition 2.2.7. *The nonlinear system Eq.2.1 is said* **hyperbolic** *in a domain $\Omega \subset \mathbb{R}^n$ if and only of the linearized system Eq. 2.5 is hyperbolic for all $U \in \Omega$.*

Finding the equivalent diagonal matrix of A and analyzing its eigenvalues is the easiest way to prove the hyperbolic behavior of the Euler's equation in 1D. Let's change the basis of A from the conservative variables $U = (\rho, \rho u, \rho E)^T$ to the primitive ones $V = (\rho, u, p)^T$; the transformation matrix $M = \partial U / \partial V$ and its inverse must be explicitly written, component by component. We have:

$$M = \begin{bmatrix} 1 & 0 & 0 \\ u & \rho & 0 \\ \frac{u^2}{2} & \rho u & \frac{1}{\gamma - 1} \end{bmatrix}, \quad M^{-1} = \begin{bmatrix} 1 & 0 & 0 \\ -\frac{u}{\rho} & \frac{1}{\rho} & 0 \\ \frac{\gamma - 1}{2} u^2 & -(\gamma - 1)u & \gamma - 1 \end{bmatrix}. \tag{2.6}$$

Proof. The demonstration is based on the same concept as in Theorem 2.2.2 and is let to the reader. □

It comes from Eq. 2.5:

$$M \frac{\partial V}{\partial t} + AM \frac{\partial U}{\partial x} = 0,$$

or, equivalently,

$$\frac{\partial V}{\partial t} + M^{-1} AM \frac{\partial U}{\partial x} = 0 \text{ or } \frac{\partial V}{\partial t} + \tilde{A} \frac{\partial U}{\partial x} = 0, \tag{2.7}$$

with

$$\tilde{A} = M^{-1} AM = \begin{bmatrix} u & \rho & 0 \\ 0 & u & \frac{1}{\rho} \\ 0 & \rho c^2 & u \end{bmatrix}, \tag{2.8}$$

and $c = \sqrt{\frac{\gamma p}{\rho}}$ is the speed of sound. Eq. 2.7 represents the Euler's equations written in a non conservative form. From Eq. 2.8, one deduces:

$$A = M \tilde{A} M^{-1} \tag{2.9}$$

It is clear that A and $\tilde{A}$ share the same eigenvalues and the computation of $det(\lambda I - \tilde{A})$ finally leads to the following diagonal matrix (composed of eigenvalues) Λ:

$$\Lambda = \begin{bmatrix} u-c & 0 & 0 \\ 0 & u & 0 \\ 0 & 0 & u+c \end{bmatrix}, \tag{2.10}$$

Using transformation matrices, we have $\tilde{A} = \tilde{R}\Lambda\tilde{R}^{-1}$ and finally:

$$A = R\Lambda R^{-1} \text{ with } R = M\tilde{R} \text{ and } R^{-1} = \tilde{R}^{-1}M^{-1} \tag{2.11}$$

One can now compute transformation matrices from A to Λ to show that all eigenvectors are real: the hyperbolic aspect of the Euler's equations will be proved. Let $\tilde{\mathcal{R}}_k, k = 1, 2, 3$ be the eigenvector at the right hand side and let $\lambda_k, k = 1, 2, 3$ be the corresponding eigenvalues. We have $\tilde{A}\tilde{\mathcal{R}}_k = \lambda_k\tilde{\mathcal{R}}_k$. Introducing Λ, $\tilde{R}$ has its k-th row composed of the eigenvectors $\tilde{\mathcal{R}}_k$ components since $\tilde{A}\tilde{R} = \tilde{R}\Lambda$. From the following choice for $\tilde{R}$:

$$\tilde{R} = \frac{1}{c^2}\begin{bmatrix} 1 & 1 & 1 \\ -c/\rho & 0 & c/\rho \\ c^2 & 0 & c^2 \end{bmatrix}, \tag{2.12}$$

we finally obtain, using Eq. 2.11:

$$R = \frac{1}{c^2}\begin{bmatrix} 1 & 1 & 1 \\ u-c & u & u+c \\ H-uc & u^2/2 & H+uc \end{bmatrix}. \tag{2.13}$$

Analogously, the left hand side eigenvectors $\tilde{\mathcal{L}}_k$ of $\tilde{A}$ are defined by $\tilde{\mathcal{L}}_k\tilde{A} = \lambda_k\tilde{\mathcal{L}}_k$ and can be computed from $\tilde{R}\tilde{R^{-1}} = Id$, which leads to:

$$\tilde{R}^{-1} = \begin{bmatrix} 0 & -\frac{\rho c}{2} & \frac{1}{2} \\ c^2 & 0 & -1 \\ 0 & \frac{\rho c}{2} & \frac{1}{2} \end{bmatrix}. \tag{2.14}$$

and

$$R^{-1} = \begin{bmatrix} \frac{1}{2}[(\gamma-1)\frac{u^2}{2} + uc] & -\frac{1}{2}[(\gamma-1)u - c] & \frac{\gamma-1}{2} \\ c^2 - (\gamma-1)\frac{u^2}{2} & (\gamma-1)u & -(\gamma-1) \\ \frac{1}{2}\left[(\gamma-1)\frac{u^2}{2} - uc\right] & -\frac{1}{2}[(\gamma-1)u + c] & \frac{\gamma-1}{2} \end{bmatrix}. \tag{2.15}$$

The extension to three-dimension flows is possible and leads to Λ as:

$$\Lambda = \begin{bmatrix} u-c & 0 & 0 & 0 & 0 \\ 0 & u & 0 & 0 & 0 \\ 0 & 0 & u & 0 & 0 \\ 0 & 0 & 0 & u & 0 \\ 0 & 0 & 0 & 0 & u+c \end{bmatrix},$$

with real eigenvectors.

Remark 2.2.8. *The eigenvalues $u - c$, u and $u + c$ represent the speed at which waves are moving in the flow. Material particles move at velocity u and acoustic waves at absolute velocities $u + c$ and $u - c$.*

Remark 2.2.9. *For a subsonic flow ($u < c$ with c sound speed), one acoustic speed is negative, which means that some information goes in a direction opposite to the flow.*

The Euler's equations being hyperbolic, discontinuous solutions can appear at a finite time. Now, we will analyze the jump at the discontinuities: Rankine Hugoniot relations give an expression for the jumps.

2.3 Strong and weak solutions of the Euler's equations

Let us work in the 2D space Ω depending on (x, t) and associated to an unstationary one-dimension flow solution of Euler equations. The transformation of a one-dimension discretization in space and time to a two-dimensions discretization in coupled time / space is chosen to follow a jump which moves in both space and time.

2.3.1 The method of characteristics and the strong solution

The method of characteristics is a mathematical technique for solving partial differential equations and in particular, it can be applied to the Euler's equations, which are first order Partial Differential Equations (PDE). In this case, the principle of the method is:

1. to transform the initial PDE into an Ordinary Differential Equation (ODE) which only involves a single variable, this transformation being possible on curves called characteristic curves,
2. to solve the ODE on the characteristic curve,
3. to transform the solution of the ODE back in the initial space to define the solution of the PDE.

For sake of simplicity, let's consider in this section the following 1D scalar Cauchy problem for which u is the unknown variable:

$$\begin{cases} \partial_t u + \partial_x f(u) = 0, \quad \forall t > 0 \\ u(0, x) = u_0(x). \end{cases} \tag{2.16}$$

Let's suppose that the initial data $x \to u_0(x)$ is $C^1(\mathbb{R})$ (continuous, derivable and with a continuous derivative). Eq. 2.16 can be written is a non conservative form:

$$\begin{cases} \partial_t u + a(t)\partial_x u = 0 \text{ with } a(u) = f'(u), \forall t > 0 \\ u(0, x) = u_0(x). \end{cases} \tag{2.17}$$

Now, let's introduce the following change of variable from (t, x) to (t', X):

$$\begin{cases} \dfrac{\partial x(t', X)}{\partial t'} = a(u(t', x(t', X))), \\ x(0, X) = X, \\ t = t' \end{cases} \tag{2.18}$$

Definition 2.3.1. *The curve $t \to x(t, X)$ defined by Eq. 2.18 is the characteristic curve in relation with the solution $t \to u(t, x)$ of Eq. 2.16.*

According to the change of coordinates origins and direction, the rules for derivatives are written as:

$$\begin{cases} \partial_{t'} = \partial_{t'} \partial t + \partial_{t'} x \partial_x = \partial_t + a \partial_x \\ \partial_X = \partial_X t \partial t + \partial_X x \partial x = J \partial x, \end{cases} \tag{2.19}$$

with $J = \partial_{X|t'} x$. One deduces from Eq. 2.19 and Eq. 2.17 that $\partial_t u + a(t)\partial_x u = 0$ and $\partial_{t'} u(t', x(t', X)) = 0$ are equivalent. As a consequence, the solution u is constant along the curves defined by $u(t', x(t', X)) = u(0, x(t', 0)) = u_0(X)$. These curves are **straight lines** and are solutions of the characteristic equation.

Theorem 2.3.2. *In 1D, for Cauchy problem Eq. 2.16, the characteristic straight line equations are:*

$$x(t, X) = X + t a(u_0(X)), \text{ with } a(u) = f'(u).$$

Theorem 2.3.3. *Let $u_0(x)$ be a continuous and differentiable except at some singular points. Suppose that the solution $x \to x(t, X)$ of the characteristic equation is continuous, differentiable except at some singular points on $[0, T] \times \mathbb{R}$ and invertible. The inverse transformation is denoted $(t, x) \to X(t, x)$ with $x(t, X(t, x)) = x$ for all $x \in \mathbb{R}$.*

Then, the function $(t, x) \to u_0(X(t, x)))$ is continuous, differentiable by pieces and is solution of the Cauchy's problem Eq. 2.16.

Definition 2.3.4. *The solutions described in Theorem 2.3.3 are called* **strong solutions**.

Remark 2.3.5. *Solving Theorem 2.3.3 is only possible for single valued problems for which characteristic lines do not cross. If characteristic lines cross, the information obtained from the characteristics can lead to the definition of a multi-valued solution or perhaps to the non existence of a solution.*

2.3.2 An example of the limited approach based on characteristics: Burgers' equation

In this section, we consider the 1D Burgers' equation coupled with an initial data:

$$\begin{cases} \dfrac{\partial u}{\partial t} + u \dfrac{\partial u}{\partial x} = 0 \\ u(x = x_0, t = 0) = u(x_0, 0) \end{cases} \tag{2.20}$$

Eq. 2.20 is called the inviscid Burgers equation since there exists an extension of Eq. 2.20 with a diffusion term. It is a nonlinear PDE which looks very close to the momentum relation of the Euler's equations.

For Burgers' equation, the characteristics are solution of $X' = u(X(t), t)$. Assume that X is a solution of this equation, then $u[X(t), t]$ is the restriction of u to this curve and along the curve:

$$\frac{d}{dt}u(X(t), t) = \frac{\partial u}{\partial x}\frac{dx}{dt} + \frac{\partial u}{\partial t} = 0. \tag{2.21}$$

We deduce from Eq. 2.21 that the solution will not change along the characteristic curve. Since the initial condition $u_0(x)$ is known, we have

$$u(X(t), t) = u(x_0, 0).$$

The right hand side is independent of t and therefore constant for the integration. We find straight lines as characteristics: $X(t) = x_0 + u(x_0, 0)t = x_0 + f(x_0)t$. The solution of the initial value problem can be written as:

$$u(x, t) = f(x_0) = f(x - ut). \tag{2.22}$$

At this level, one can notice that

1. the solution is not given explicitly through Eq. 2.22,
2. the characteristic are straight lines but they do not share the same slope,
3. as a consequence, depending on the initial position and on $f(x_0)$, the characteristic lines may intersect. In this case, an analysis of the problem can lead to the existence of several solutions or to the no-existence of a solution to the initial problem.

To overcome this lack of existence of a classical solution, we must introduce a broader notion of a solution, a weak solution.

2.3.3 Strong and weak solution

Roughly speaking, a weak solution may contain discontinuities, may not be differentiable, and will require less smoothness to be considered as solution than a classical strong solution. Working with the weak solution of a PDE usually requires that the PDE be reformulated in an integral form. If a classical solution to the problem exists, it will also satisfy the definition of a weak solution.

Let Ψ be the space of C^1 functions ϕ with zero values out of Ω and on the boundary $\partial\Omega$. Then, if U is a strong solution of Euler equations, we have:

$$\int_\Omega \left[U\frac{\partial \phi}{\partial t} + F(U)\frac{\partial \phi}{\partial x} \right] = 0, \quad \forall \phi(x, t) \in \Psi.$$

U is then said to be a weak solution of Euler equations Eq. 2.1.

Proof. The proof is straightforward. Multiply formally Eq. 2.1 by ϕ, integer on Ω and use Green Formula. □

One can also show that if U is a weak solution, U can be also a strong solution: the reciprocity is true is the weak solution is regular (typically C^1). As a consequence, both approaches can be equivalent. However, a weak formulation is a more general concept than the strong solution.

Rankine Hugoniot jump relations

Let a discontinuity be defined in the space (x,t). The discontinuity divides an open space Ω in two open spaces Ω_1 and Ω_2, such as shown in Fig. 2.1. Let ∂X denote the boundary of a space X. Let C be the curve of separation between Ω_1 et Ω_2.

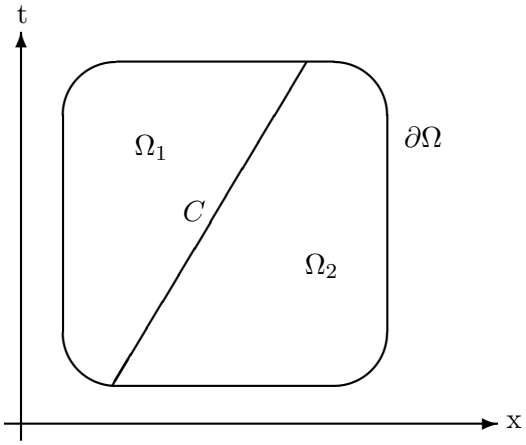

Figure 2.1: *Definition of Ω as a coupled space / time domain.*

The weak formulation of Euler's equations in 1D is written as:

$$\sum_{i=1}^{2}\left(\int_{\Omega_i}\left[U\frac{\partial\phi}{\partial t}+F(U)\frac{\partial\phi}{\partial x}\right]\right)=0,\quad\forall\phi(x,t)\in\Psi. \tag{2.23}$$

By continuity of U in both spaces Ω_1 and Ω_2, Eq 2.23 can be transformed by Green formula on each subspace. It leads to:

$$\sum_{i=1}^{2}\left(\int_{\partial\Omega_i}[\phi U n_{i,t}+F(U)\phi n_{i,x}]\right)=\sum_{i=1}^{2}\left(\int_{\Omega_i}\left[\phi(\frac{\partial U}{\partial t}+\frac{\partial F(U)}{\partial x})\right]\right),\quad\phi(x,t)\in\Psi. \tag{2.24}$$

Since U is a weak solution of Euler equations, the right hand side of Eq 2.24 is zero. The left hand side of Eq 2.24 can be formulated in another way by the change of volume integrals in boundary ones on $\partial\Omega\cup C$. Using the fact that $\forall\phi\in\Psi$, $\phi=0$ on $\partial\Omega$, one obtains:

$$\sum_{i=1}^{2}\left(\int_{C}[(Un_{i,t}+F(U)n_{i,x})\phi]\right)=0. \tag{2.25}$$

On the discontinuity, $\vec{n_2}=-\vec{n_1}$ and if U_1 and U_2 are the values of U in Ω_1 et Ω_2, we have:

$$\int_{C}[(U_1-U_2)n_{1,t}+(F(U_1)-F(U_2))n_{1,x})\phi]=0. \tag{2.26}$$

Since Eq. 2.26 is true for any function ϕ of class C^1 with a compact support, the final Rankine Hugoniot's jump expression is simply:

$$(U_1-U_2)n_{1,t}+(F(U_1)-F(U_2))n_{1,x}=0. \tag{2.27}$$

At this level, we recall that n_1 is the unit normal vector on C directed outward Ω_1 and it has two components following the (x,t) space direction.

2.3.4 Non uniqueness of the weak solution

Here, the aim is not to present the whole details of the mathematical background and we simply want to justify that there may be several weak solutions of the initial problem. The weak solution is defined as a solution of an integral formulation with respect to the classical measure in $\mathbb{R}^k$ (Lebesgues measure). Let us suppose (without lack of generality for the present purpose) that the solution is look for in $\mathbb{R}$. Let us introduce the Dirac function $\delta_{x_0}(x) = 0$ is $x \neq x_0$, 1 else. Then, if f is a weak solution, $f + \delta_{x_0}$ is also a solution. The proof is linked with the fact that the Dirac function δ_{x_o} is not seen by the Lebesgues' measure:

$$\int_\Omega \delta_{x_0}(x)dx = 0, \forall x_0 \in \mathbb{R}\,.$$

A simple extrapolation of this idea justifies that the weak formulation of the Euler's equation in 1D have several solutions. If one finds a solution f, then another (different) solution is simply $f + \delta_{x_0}$.

As a conclusion, the weak formulation considers a space of weak solutions larger than the one of strong solutions composed of continuous and differentiable functions. For an initial solution which corresponds to the strong solution, the weak formulation can add one or more than one new solutions. The question is now to choose the legitimate one. To do so, mathematician introduce the notion of entropy (not necessary the same as for fluids!). A new criterium on the (mathematical) entropy enables to select one solution in the space of weak solutions. This solution will be the general solution which we look for.

The definition of the mathematical entropy is not in the purpose in such a course on numerical schemes. If interested, the reader is suggested to read Despres books [1] (in French).

2.3.5 Riemann problem

Definition 2.3.6. *The Riemann problem for Euler equations in one dimension consists in finding a (weak) solution to the Euler equations with an initial condition defined by:*

$$U(x,0) = \begin{cases} U_L & \forall x < 0 \\ \\ U_R & \forall x > 0. \end{cases} \tag{2.28}$$

In other words, the principle is to analyze the behavior of the solution in presence of a discontinuity. Of course, it is exactly the model problem found on an interface during the finite volume process.

The Euler equations coupled with the initial condition Eq. 2.28 does not include any time or space scale: if $u(x,t)$ is a solution, then $u(\alpha x, \alpha t)$ is solution, whatever α is. This is called a self-similar solution. The concept of self-similar solution means that the solution only depends on x/t and is therefore constant on the half-lines which cross $(0,0)$.

The analysis of the solution behavior can be conducted directly through the study of Rankine Hugoniot jump relations, Without entering in details, the discontinuities can be identified precisely. In practice, it is possible to go further in the development since the Rieman's problem solved with Rankine Hugoniot relations is a foundation of numerical schemes. This topic will be analyzed in chapter 4 of this document.

Chapter 3

Numerical schemes built from mathematical considerations

This chapter is mainly devoted to the analysis of the Jameson Schmidt Turkel convection scheme [2]. After introducing some possibilities to define the numerical scheme for convection, the JST scheme is introduced and its stabilization terms explained.

3.1 Introduction

We have seen in chapter 2 the hyperbolic aspect of Euler equations, Rankine Hugoniot jumps and the non uniqueness of weak solutions. In this chapter, simply forget all the lessons and take the point of view of a very young mathematician.

For sake of clarity in introducing the underlying approach, let us consider the simple advection equation at velocity a in 1D:

$$\frac{\partial u}{\partial t} + a\frac{\partial u}{\partial x} = 0. \tag{3.1}$$

Integrate Eq. 3.1 as for the Finite Volume approach leads to:

$$\frac{d}{dt}\left(\int_\Omega u\right) + a\int_{\partial\Omega} u.\vec{n}ds = 0. \tag{3.2}$$

The difficulty concerns the definition of the velocity u at the interface for the boundary integral in Eq. 3.2. For this simple case, why could not we choose $u = 0.5(u_L + u_R)$ which is the mean between left and right values states around the interface? This kind of scheme is called a centered scheme since there is the same kind of contribution for left and right hand sides fields. For Euler equations, the approach is a bit more complex due to the nonlinear terms.

3.2 Some consequences of non linearity

The convection terms within the Navier Stokes equations are nonlinear. In particular, the nonlinear part of the convection flux depends on choices for $H = (\vec{u}\nabla).\vec{u}$. We have seen in chapter 1 that H can also be written as $H = \nabla.\vec{u}\otimes\vec{u}$. There are mainly four possibilities to express H or its components:

1. The divergence form:

$$H_l = \frac{\partial u_l u_m}{\partial x_m}, \tag{3.3}$$

2. The skew-symmetric form:

$$H_l = \frac{1}{2}\left(\frac{\partial u_l u_m}{\partial x_m} + u_m \frac{\partial u_l}{\partial x_m}\right), \tag{3.4}$$

3. the convection form:

$$H_l = u_m \frac{\partial u_l}{\partial x_m}, \tag{3.5}$$

4. the rotational form:

$$H_l = u_m \left(\frac{\partial u_l}{\partial x_m} - \frac{\partial u_m}{\partial x_l}\right) + \frac{1}{2}\frac{\partial u_m u_l}{\partial x_l}. \tag{3.6}$$

From now on, let l / r denote respectively the left / right volumes on both sides of an interface i. The interface flux F is an integral which is discretized as a product of a flux density $\mathcal{F}$ and a normal unit vector $\vec{n}$. For centered schemes, the interface flux density can be computed:

- using the mean of the conservative variables at the interface:

$$\mathcal{F}_i = \mathcal{F}\left(\frac{1}{2}(W_l + W_r)\right). \tag{3.7}$$

  This is the typical formulation proposed by Jameson *et al.* [2].

- using the mean of the flux at the interface:

$$\mathcal{F}_i = \frac{1}{2}\Big(\mathcal{F}(W_l) + \mathcal{F}(W_r)\Big). \tag{3.8}$$

3.2.1 Analysis of differences between mean of variables and mean of flux for a centered convection scheme

The difference between both expressions for the interface flux can be analyzed easily using Taylor expansion on the following one-dimension nonlinear equation $\partial u/\partial t + \partial u^2/\partial x = 0$. From now on, a volume is defined by its index i and the interface index $i + 1/2$ is located between volumes I and $I + 1$. The semi-discrete Finite Volume discrete formulation can be written:

$$V\frac{\partial u}{\partial t} + F_{i+1/2} - F_{i+1/2} = \Delta x \frac{\partial u}{\partial t} + F_{i+1/2} - F_{i+1/2} = 0. \tag{3.9}$$

In Eq. 3.9, $\Delta x = V$ represents the length of the segment which defines the control volume.

If the flux F is computed with Eq. 3.7, one has:

$$\frac{\partial u}{\partial t} + \frac{1}{\Delta x}\left[\left(\frac{u_{i+1} + u_i}{2}\right)^2 - \left(\frac{u_i + u_{i-1}}{2}\right)^2\right] = \frac{\partial u}{\partial t} + \frac{1}{2}\left(\frac{u_{i+1}^2 - u_i^2}{2\Delta x} + 2u_i\frac{u_{i+1} - u_{i-1}}{2\Delta x}\right) = 0. \tag{3.10}$$

Using Taylor expansions, one can easily prove from Eq. 3.10 that the discretization error is:

$$\frac{1}{2}\left(\frac{u_{i+1}^2-u_i^2}{2\Delta x}+2u_i\frac{u_{i+1}-u_{i-1}}{2\Delta x}\right)-\frac{\partial u^2}{\partial x}=\frac{1}{6}\frac{\partial^3 u^2}{\partial x^3}(\Delta x)^2-\frac{1}{2}\frac{\partial u}{\partial x}\frac{\partial^2 u}{\partial x^2}(\Delta x)^2+O\left((\Delta x)^4\right). \quad (3.11)$$

If the flux F is computed with Eq. 3.8, one has:

$$\frac{\partial u}{\partial t}+\frac{u_{i+1}^2-u_i^2}{2\Delta x}=0, \quad (3.12)$$

and using Taylor expansions, one deduces from Eq. 3.12 that the numerical error is centered for the first order derivative $\partial/\partial x$:

$$\frac{u_{i+1}^2-u_i^2}{2\Delta x}-\frac{\partial u^2}{\partial x}=\frac{1}{6}\frac{\partial^3 u^2}{\partial x^3}(\Delta x)^2+O\left((\Delta x)^4\right). \quad (3.13)$$

The difference between the considered approximations Eq. 3.11 and Eq. 3.13 is the second order term $-\frac{1}{2}\frac{\partial u}{\partial x}\frac{\partial^2 u}{\partial x^2}(\Delta x)^2$ which gives a diffusive or anti diffusive correction according to the sign of $\partial u/\partial x$. Kravchenko and Moin [3] proved that the skew-symmetric form leads to a lower aliasing error and that the divergence form is less dissipative, which can drive to a non conservation of energy.

3.3 The Jameson's artificial dissipation

The centered scheme is unstable and must be used in combination with an artificial dissipation. The artificial dissipation is a blending between second and fourth order dissipation terms. For the Finite Volume discretization, the conservation is guaranteed by introducing the dissipation term directly in the flux expression $F_{i+1/2}=\mathcal{F}_{i+1/2}\vec{n}-d_{i+1/2}$ with:

$$d_{i+1/2}=\varepsilon^{(2)}_{i+1/2}(W_{i+1}-W_i)-\varepsilon^{(4)}_{i+1/2}(W_{i+2}-3W_{i+1}+3W_i-W_{i-1}). \quad (3.14)$$

The coefficients $\varepsilon^{(2)}_{i+1/2}$ and $\varepsilon^{(4)}_{i+1/2}$ change the importance of the dissipation term according to the physics. Both terms depend on the scale factor $r_{i+1/2}$:

$$\begin{cases}\varepsilon^{(2)}_{i+1/2} & = k^{(2)}r_{i+1/2}\nu_{i+1/2}\\ \varepsilon^{(4)}_{i+1/2} & = max(0,k^{(4)}r_{i+1/2}-\varepsilon^{(2)}_{i+1/2}).\end{cases} \quad (3.15)$$

The factor $r_{i+1/2}$ is computed from the spectral radius r_i of the Jacobian matrix $A=\partial\mathcal{F}.\vec{n}/\partial W$ (estimated from the mean surface normal vector $(\vec{n}_{i+1/2}+\vec{n}_{i-1/2})/2$) in the cell i according to the following relations:

$$r_{i+1/2}=\frac{r_i+r_{i+1}}{2}. \quad (3.16)$$

Finally, $\nu_{i+1/2}$ from Eq. 3.15 is built with a normalized second order pressure sensor:

$$\mu_i=\left|\frac{p_{i+1}-2p_i+p_{i-1}}{p_{i+1}+2p_i+p_{i-1}}\right| \text{ and } \nu_{i+1/2}=max(\mu_i,\mu_{i+1}). \quad (3.17)$$

In fact, the term in $\varepsilon^{(2)}$ is generally a second order term but in regions of strong pressure gradients, it becomes a first order term only. Near shocks, the term in $\varepsilon^{(2)}$ represents the main dissipation contribution. However, this term does not remove completely numerical oscillations and it stays waves on about 1% of the density which limits strongly the convergence to the steady state. These waves are finally destroyed by the introduction of the fourth order term which adds dissipation in the whole computational domain. However, this fourth order dissipation term also makes oscillations appear near shocks and the fourth order dissipation term must be destroyed in regions where $\varepsilon^{(2)}$ is high, which explains the form of Eq. 3.15.

For transonic RANS computations, classical choices are:

$$0.5 < k^2 < 1 \text{ and } 0.01 < k^{(4)} < 0.03\,,$$

while for subsonic flows, the second order dissipation coefficient can be chosen equal to 0. For incompressible flows, the choice of the coefficients $k^{(2)}$ and $k^{(4)}$ must be done carefully in order not to avoid an introduction of a numerical dissipation at the same order as the natural fluid dissipation issued from diffusion.

3.4 Default of the approach

The Jameson Schmidt Turkel's scheme is defined as a pure centered scheme combined with dissipation terms issued from mathematical analysis and physical considerations. Numerical experiences have shown that the JST scheme is not sufficiently robust to treat strong shocks (typically for a Mach number higher than 2) and there exists another class of schemes -upwind schemes- which work better for such configurations. They are introduced in Chapter 4.

Chapter 4

Upwind schemes for Euler equations

4.1 Introduction

All central space discretizations, Jameson Schmidt Turkel as an example, have a symmetry with respect to a change in sign of the Jacobian eigenvalues, and physically speaking are not able to distinguish between upstream and downstream influences. This means that the physical propagation of perturbations along characteristics (hyperbolic behavior of the equations) is not taken into account in central space discretizations. This lack of physics can be clearly seen when discontinuities appear in the flow (shock waves, surface discontinuities...) under the form of oscillations. For example, oscillations appear when using a central second order scheme in vicinity of a shock wave, and thus artificial dissipation terms are added to stabilize the solution. The objective of this chapter is to present the way to introduce physical behavior in discretization schemes.

In this chapter, we consider the mono-dimensional Euler equation written in conservative form:

$$\frac{\partial U}{\partial t} + \frac{\partial F(U)}{\partial x} = 0 \tag{4.1}$$

The initial solution U at $t = 0$ is supposed known and is denoted $U(x, 0), \forall x \in [0, L]$. The goal is to find a numerical approximation of the solution $U(x, t)$. Eq. 4.1 will be discretized with a Finite Volume approach and to do that, $[0, L]$ is divided into M finite volumes (segment in this mono-dimensional case) defined by:

$$x_{i-1/2} \leq x \leq x_{i+1/2}, \tag{4.2}$$

The extreme values $x_{i-1/2}$ and $x_{i+1/2}$ of the cell I_i define the position of the inter-cell boundary at which the corresponding interface numerical fluxes must be specified. We recall, namely, that the finite volume discretization of Eq. 4.1, is expressed as:

$$\frac{\partial \widehat{U}_i}{\partial t} + \frac{F_{i+1/2} - F_{i-1/2}}{x_{i+1/2} - x_{i-1/2}} = 0 \tag{4.3}$$

where

$$\widehat{U}_i = \int_{x_{i-1/2}}^{x_{i+1/2}} U dx, \tag{4.4}$$

represent the mean value on the cell i, and $F_{i+1/2}$ is the flux through the interface $i + 1/2$. The numerical scheme is the discrete operator which defines the way to compute this flux.

4.2 Flux Vector Splitting schemes

The first and easier way to introduce physical principle in the construction of numerical fluxes is to take into accounts the sign of the characteristic wave. By using the characteristic decomposition of Jacobian matrix as seen in 2.2.2, the Euler equations can be put in characteristic form:

$$\frac{\partial W}{\partial t} + \Lambda \frac{\partial W}{\partial x} = 0, \tag{4.5}$$

where W represents the characteristic variables defined by:

$$\partial W = R^{-1} \partial U. \tag{4.6}$$

Λ is a diagonal matrix, and the terms of the diagonal are the eigenvalues of the Jacobian. The set of eigenvalues are split into two parts

$$\Lambda = \Lambda^+ + \Lambda^-, \tag{4.7}$$

with the property that all values of Λ^+ (resp. Λ^-) are positive (resp. negative). Since $F(U)$ is a homogeneous function of degree one in U, one has:

$$F(U) = AU = R\Lambda R^{-1} U, \tag{4.8}$$

and the following flux splitting can be defined:

$$F^+ = A^+ U, \quad F^- = A^- U \text{ with } A^+ = R\Lambda^+ R^{-1} \text{ and } A^- = R\Lambda^- R^{-1}. \tag{4.9}$$

A general calculation for an arbitrary splitting is simply defined by

$$\Lambda^\pm = \begin{bmatrix} \lambda_1^\pm & 0 & 0 \\ 0 & \lambda_2^\pm & 0 \\ 0 & 0 & \lambda_3^\pm \end{bmatrix} \tag{4.10}$$

with the eigenvalues $\lambda_1 = u - c$, $\lambda_2 = u$ and $\lambda_3 = u + c$. A general expression for F can then be found and it is written:

$$F^\pm = \frac{\rho}{2\gamma} \begin{bmatrix} 2(\gamma-1)\lambda_2^\pm + \lambda_1^\pm + \lambda_3^\pm \\ 2(\gamma-1)u\lambda_2^\pm + \lambda_3^\pm (u+c) + \lambda_1^\pm (u-c) \\ (\gamma-1)u^2\lambda_2^\pm + \frac{\lambda_3^\pm}{2}(u+c)^2 + \frac{\lambda_1^\pm}{2}(u-c)^2 + \frac{3-\gamma}{2(\gamma-1)}c^2(\lambda_1^\pm + \lambda_3^\pm) \end{bmatrix} \tag{4.11}$$

and finally:

$$F_{i+1/2} = F_i^+ + F_{i+1}^-. \tag{4.12}$$

In 1D, and with the notations which have been introduced, Eq. 4.12 means that the interface flux at $i + 1/2$ is the sum of the contribution from the cell i for waves going from left to right, and from the cell $i + 1$ for waves going from right to left.

The decomposition Eq. 4.7 is not unique, and two forms will be given. The first one is due to Steger and Warming [7] and is defined by:

$$\lambda_k^+ = \frac{\lambda_k + |\lambda_k|}{2} \tag{4.13}$$

$$\lambda_k^- = \frac{\lambda_k - |\lambda_k|}{2}. \tag{4.14}$$

The second one has been proposed by Steger in 1978 [6]:

$$\lambda_2^+ = \frac{u + |u|}{2} \quad , \quad \lambda_2^- = \frac{u - |u|}{2} \tag{4.15}$$

$$\lambda_1^+ = \lambda_2^+ \quad , \quad \lambda_1^- = \lambda_2^- - c \tag{4.16}$$

$$\lambda_3^+ = \lambda_2^+ + c \quad , \quad \lambda_3^- = \lambda_2^-. \tag{4.17}$$

When the velocity is sonic ($u = \pm c$), $\lambda_1^\pm$ and $\lambda_3^\pm$ become 0 for the first decomposition, which is not the case for the second one. This difference generates a discontinuity in an expansion flow when the velocity reaches c. One can notice that the Jacobian $\frac{\partial F^+}{\partial U} \neq A^+$ and the eigenvalues of this Jacobian are different from those of A^+. However, Steger and Warming reported that $\frac{\partial F^+}{\partial U}$ has just positive eigenvalues. This scheme could be interpreted as presented in Fig. 4.1, with the direction of the information following the sign of f (positive or negative):

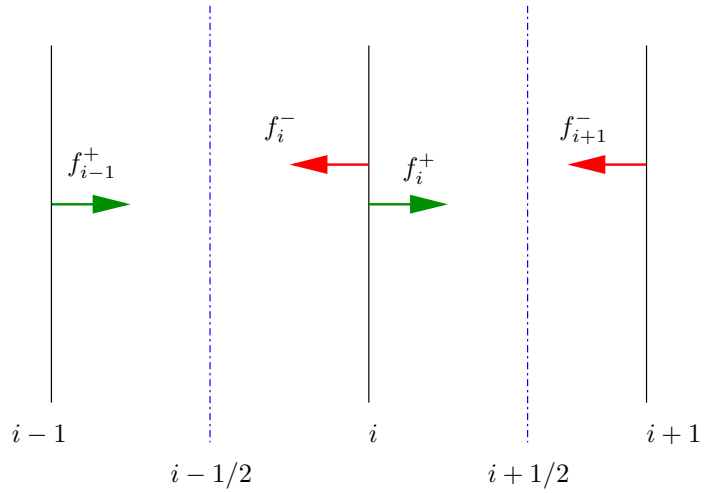

Figure 4.1: direction of waves according to the sign of the Jacobian eigenvalues.

4.3 Schemes based on the Riemann's solver

4.3.1 Basic first order scheme

The first step consists in introducing a piecewise constant approximation of the solution $U(x,t)$. More precisely, the function $U(x,t)$ is assumed constant on each segment $[x_{i-1/2}, x_{i+1/2}]$ and

its (mean) value is $\widehat{U(t)}$. Since all flows have quantities which vary in space (and eventually in time), it is not possible to represent a flow on each control volume by a unique value for all conservative fields. Therefore, as presented in Fig. 4.2, there must exist a discontinuity at each mesh interface. Finally, this discontinuity is solved with the solution of the so-called *Riemann problem* and the solution of this problem gives a way to compute the numerical flux at mesh interfaces.

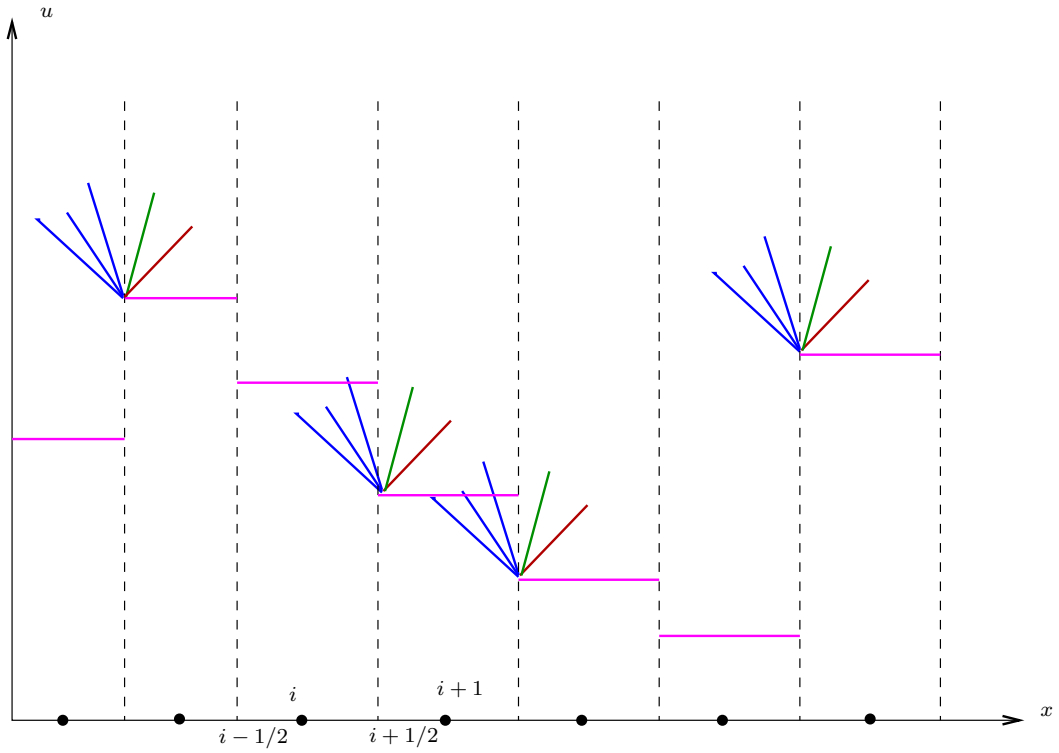

Figure 4.2: Example of a discontinuous (mean) solution on a mesh.

4.3.2 Riemann problem

The Riemann's problem for the one-dimensional time-dependent Euler's equation is the Initial Value Problem (IVP) for the conservation law given by Eq. 4.1, with the following initial condition:

$$U(x,0) = \begin{cases} U_L & \text{if} \quad x < 0, \\ U_R & \text{if} \quad x > 0. \end{cases} \tag{4.18}$$

The domain of interest in the $x - t$ plane are points (x,t) with $-\infty < x < +\infty$ and $t > 0$. Physically, the Riemann's problem is a slight generalization of the so called *shock-tube problem*: two motionless gases ($u_L = u_R = 0$) in a tube are separated by a diaphragm and the diaphragm breaking generates a wave system that typically consists of a rarefaction wave, a contact discontinuity and a shock wave[1]. Each wave generated at $t = 0$ is associated with one of the

[1] When the velocities are not zero, different wave associations could occur.

three eigenvalues $u-c$, u, $u+c$. Note that the speeds of these waves are not, in general, the characteristics speeds given by the eigenvalues. As an example, a shock wave result of the focusing (the superimposition) of acoustic waves which propagate with the velocity equal to $u+c$ or $u-c$, but the speed of the resulting shock wave is completely different and depends purely on the initial condition.

The Riemann's problem could be exactly resolved and let $RP(U_L, U_R)$ denote the solution of the Riemann's problem between the two states U_L and U_R. The Riemann's problem solution is self-similar, which means that if $u(x,t)$ is a solution, then $u(\alpha x, \alpha t)$ is also solution, whatever α is. The concept of self-similar solution lies simply with the fact that the solution only depends on x/t and is therefore constant on the half-lines which cross $(0,0)$ in $(x-t)$ plane.

4.3.3 From the Riemann's problem to numerical flux integration

The temporal integration of Eq. 4.3 could be done by several techniques such as simple backward Euler or Runge Kutta. For all methods, a sub-step consists in computing the solution at time $t+\Delta t$. Δt represents either the time step or the sub-step time of a Runge Kutta method. To simplify the purpose, only the backward Euler method is considered, and only the one-step Runge Kutta explicit time integration is considered, and thus Eq. 4.3 becomes:

$$\widehat{U}_i^{n+1} = \widehat{U}_i^n - \frac{\Delta t}{x_{i+1/2} - x_{i-1/2}} \left[F_{i+1/2} - F_{i-1/2} \right]. \tag{4.19}$$

$\widehat{U}_i^n$ represents an approximation of mean value on cell I_i of the function $U(x,t_n)$ at time $t_n = n\Delta t$. In this case, do not forget that the fluxes at computed with the solution at time $n+1$.

The only remaining problem is to determinate the numerical fluxes $F_{i+1/2}$. To do this, Godunov proposed to evaluate an approximation of the state vector at temporal step $n+1$ by using the two Riemann's problem at interfaces $i-1/2$ and $i+1/2$. He proposed that:

$$\widehat{U}_i^{n+1} = \frac{1}{\Delta x} \left[\int_0^{\Delta x/2} RP(\widehat{U}_{i-1}, \widehat{U}_i) \left(\frac{x}{\Delta t} \right) dx + \int_{-\Delta x/2}^{0} RP(\widehat{U}_i, \widehat{U}_{i+1}) \left(\frac{x}{\Delta t} \right) dx \right] \tag{4.20}$$

where $\Delta x = x_{i+1/2} - x_{i-1/2}$.

This formulation is easy to understood for the linear convection equation:

$$\frac{\partial u}{\partial t} + au = 0 \quad a > 0. \tag{4.21}$$

The solution of the Riemann's problem associated with Eq. 4.21 corresponds simply to a translation of the discontinuity at speed a, as described in Fig. 4.3. Thus, with the notations used before:

$$RP(u_{i-1}, u_i) = \begin{cases} u_{i-1}^n & if \quad x/t < a, \\ u_i^n & if \quad x/t > a, \end{cases} \tag{4.22}$$

Likewise, the solution at interface $i+1/2$ is given by:

$$RP(u_i, u_{i+1}) = \begin{cases} u_i^n & if \quad x/t < a, \\ u_{i+1}^n & if \quad x/t > a, \end{cases} \tag{4.23}$$

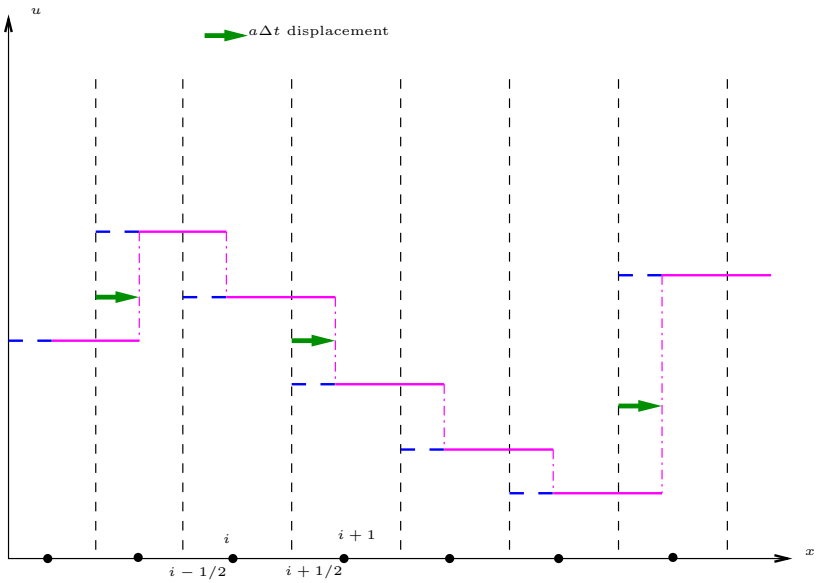

Figure 4.3: Description of the evolution of the solution of the linear convection equation Eq. 4.21.

The formulation Eq. 4.20 could be written as:

$$u_i^{n+1} = \frac{1}{\Delta x}\left[a\Delta t u_{i-1}^n + (\Delta x - a\Delta t)u_i^n\right], \tag{4.24}$$

which is equivalent to:

$$u_i^{n+1} = u_i^n - a\frac{\Delta t}{\Delta x}\left(u_i^n - u_{i-1}^n\right). \tag{4.25}$$

The first order upwind scheme could be recognized, and the CFL restriction expresses simply that the discontinuity which is localized at interface $i-1/2$ at time t_n does not leave the cell I_i during Δt, which reads:

$$a\Delta t < \Delta x. \tag{4.26}$$

To obtain the formulation in term of numerical fluxes, we use the following property of conservation law:

$$\int_{x_1}^{x_2} U(x,t_2)dx = \int_{x_1}^{x_2} U(x,t_1)dx + \int_{t_1}^{t_2} F(U(x_1,t))dt - \int_{t_1}^{t_2} F(U(x_2,t))dt \tag{4.27}$$

for any control volume $[x_1,x_2]\cdot[t_1,t_2]$. This relation results from the integration of Eq. 4.1 over the volume $[x_1,x_2]\cdot[t_1,t_2]$. If $\tilde{U}(x,t)$ represents the superimposition of $RP(\widehat{U}_{i-1},\widehat{U}_i)$ and $RP(\widehat{U}_i,\widehat{U}_{i+1})$, the Godunov's formula reduces to:

$$\widehat{U}_i^{n+1} = \frac{1}{\Delta x}\left[\int_{x_{i-1/2}}^{x_{i+1/2}} \tilde{U}(x,t_{n+1})dx\right]. \tag{4.28}$$

By using Eq. 4.27 in which $x_1 = x_{i-1/2}$, $x_2 = x_{i+1/2}$, $t_1 = t_n$ and $t_2 = t_{n+1}$, it comes:

$$\widehat{U}_i^{n+1} = \widehat{U}_i^n + \int_0^{\Delta t} F\left[RP(\widehat{U}_{i-1}, \widehat{U}_i)(x_{i-1/2}, t)\right] dt - \int_0^{\Delta t} F\left[RP(\widehat{U}_i, \widehat{U}_{i+1})(x_{i+1/2}, t)\right] dt \quad (4.29)$$

Note that $RP(\widehat{U}_i, \widehat{U}_{i+1})(x_{i+1/2}, t)$ corresponds to the time evolution at interface $x_{i+1/2}$ of the Riemann's problem solution $RP(\widehat{U}_i, \widehat{U}_{i+1})$ which is centered around $x_{i+1/2}$, and thus corresponds to the solution along the ray $x/t = 0$ and so:

$$RP(\widehat{U}_i, \widehat{U}_{i+1})(x_{i+1/2}, t) = RP(\widehat{U}_i, \widehat{U}_{i+1})(0). \quad (4.30)$$

Finally, we obtain the following formulation for the numerical flux:

$$F_{i+1/2} = F\left[RP(\widehat{U}_i, \widehat{U}_{i+1})(0)\right], \quad (4.31)$$

which is called the Godunov's scheme.

4.3.4 The Godunov's scheme for a scalar equation

For the scalar nonlinear equation coupled with the following initial conditions:

$$\frac{\partial u}{\partial t} + \frac{\partial f(u)}{\partial x} = 0, \text{ with } u(x,0) = \begin{cases} u_L & if \quad x < 0 \\ u_R & if \quad x > 0, \end{cases} \quad (4.32)$$

the Godunov's scheme is:

$$f_{1/2} = \begin{cases} \min\limits_{u_L < u < u_R} f(u) & if \quad u_L < u_R \\ \max\limits_{u_R < u < u_L} f(u) & else \end{cases} \quad (4.33)$$

For the Burgers' equation in which the function takes the nonlinear expression $f(u) = u^2/2$, one can prove that:

$$f_{1/2} = \max\left[\frac{1}{2}(u_R^-)^2, \frac{1}{2}(u_L^+)^2\right] \quad (4.34)$$

where $u^+ = \max(u, 0)$ and $u^- = \min(u, 0)$.

4.4 Approximate Riemann solver

The method of Godunov is very attractive because it enables the computation of numerical fluxes according to the properties of the Euler equations. The Godunov's scheme is based on exact solutions of the Euler's equations, but a major drawback lies in the requirement of the Riemann's problem solution at each control volume interface. Finally, the method is CPU time consuming and many simplified version have been published in the literature with the goal to diminish the CPU time for solving the Riemann's problem. In practice, all methods are based on simplifications of the Riemann's problem obtained by modifying the waves system in the Riemann's solver, leading to a two shock waves scheme or a two rarefaction waves scheme. An approximation of $RP(U_L, U, R)$ is find and thus the Godunov's scheme is used to compute the numerical fluxes.

The most famous approximated Riemann's solver is the Roe's scheme, a Riemann's solver for linear system of equations.

4.4.1 Roe scheme

The principle is to approximate the nonlinear conservative law by a linearized form. Introducing the Jacobian matrix $A = \frac{\partial F}{\partial U}$, and using the derivative rule[2], the conservation laws

$$\frac{\partial U}{\partial t} + \frac{\partial F(U)}{\partial x} = 0$$

is transformed in:

$$\frac{\partial U}{\partial t} + A(U)\frac{\partial U}{\partial x} = 0. \tag{4.35}$$

Roe [5] replaced the Jacobian matrix $A(U)$ by a **constant** matrix:

$$\tilde{A} = \tilde{A}(U_L, U_R), \tag{4.36}$$

which is a function of the data states U_L, U_R. The original Riemann's problem is then replaced by the following approximated Riemann's problem:

$$\begin{cases} \frac{\partial U}{\partial t} + \tilde{A}\frac{\partial U}{\partial x} = 0 \\ U(x,0) = \begin{cases} U_L & if \quad x < 0 \\ U_R & if \quad x > 0. \end{cases} \end{cases} \tag{4.37}$$

Eq. 4.37 is then solved exactly. The Roe's Jacobian matrix $\tilde{A}$ is required to satisfy:

- $\tilde{A}(U_L, U_R)(U_R - U_L) = F(U_R) - F(U_L)$ for conservation,
- $\tilde{A}$ must be diagonalizable, with real eigenvalues,
- $\tilde{A}(U, U) = A(U)$ where A is the Jacobian matrix of F with respect to U : $A = \partial F / \partial U$.

One can prove that the Roe's matrix $\tilde{A}$ is identical to the matrix $A(\tilde{U})$ where the mean state $\tilde{U}$ is called the Roe's average and is defined by:

$$a = \sqrt{\frac{\rho_R}{\rho_L}}, \quad \tilde{\rho} = a\rho_L$$

$$\tilde{u} = \frac{u_L + a u_R}{1 + a}, \quad \tilde{H} = \frac{H_L + a H_R}{1 + a}$$

with u velocity component and H total enthalpy.

The Riemann's problem for a system of linear equations must now be solved. The jump between the states vectors U_R and U_L is projected onto the right hand-sided eigenvectors:

$$\Delta U = U_R - U_L = \sum_{l=1}^{3} \alpha_l R_l \tag{4.38}$$

[2] Another technique is presented in [1] and it seems better written but does not correspond to the classical approach proposed in the litterature.

where R_l represents the l^{th} column of matrix R, and $\alpha = R^{-1}\Delta U$ is the vector of characteristic waves strengths. The solution of the linearized Riemann's problem evaluated along the $t-$axis $(x/t = 0)$ is given by:

$$LRP(U_L, U_R)(0) = U_L + \sum_{\lambda_l \leq 0} \alpha_l R_l = U_R - \sum_{\lambda_l \geq 0} \alpha_l R_l \tag{4.39}$$

Using directly Eq. 4.31, it follows that ($F_{1/2}$ represents the flux at interface between the two states U_L and U_R):

$$F_{1/2} = \tilde{A}U_L + \sum_{\lambda_l \leq 0} \alpha_l \lambda_l R_l = \tilde{A}U_R + \sum_{\lambda_l \geq 0} \alpha_l \lambda_l R_l \tag{4.40}$$

To find a numerical flux formulation, the process is the same as for the Godunov's scheme: an integration over the two domains $[-M, 0] \cdot [0, \Delta t]$ and $[0, M] \cdot [0, \Delta t]$ leads to the following relations:

$$\Delta t F^L_{1/2} = \Delta t F_L - MU_L - \int_{-M}^{0} LRP(U_L, U_R)(x, \Delta t)dt \tag{4.41}$$

$$\Delta t F^R_{1/2} = \Delta t F_R - MU_R + \int_{0}^{M} LRP(U_L, U_R)(x, \Delta t)dt \tag{4.42}$$

where:

- $LRP(U_L, U_R)$ represents the linearized Riemann problem's solution,
- $F^L_{1/2}$ and $F^R_{1/2}$ are respectively the fluxes at $x = 0$ for the left hand sides $x \to 0^-$ (resp. right hand side $x \to 0^+$) of the interface.

If one considers the difference $F^R_{1/2} - F^L_{1/2}$, it comes:

$$F^R_{1/2} - F^L_{1/2} = \Delta t(F_R - F_L) - M(U_L - U_R) + \int_{-M}^{M} LRP(U_L, U_R)(x, \Delta t)dt \tag{4.43}$$

For the (exact) solution of the exact Riemann's problem in the Euler's equations context, the right hand side of Eq. 4.43 would be 0. In the present linearized approximation, a solution of the linearized Euler's equations $LRP(U_L, U_R)$ is not a solution of the nonlinear initial equations. Remembering the first property of the Roe's matrix $\tilde{A}$, one has $F_R - F_L = \tilde{A}(U_R - U_L)$, and so Eq. 4.43 becomes:

$$F^R_{1/2} - F^L_{1/2} = \Delta t(\tilde{A}U_R - \tilde{A}U_L) - M(U_L - U_R) + \int_{-M}^{M} LRP(U_L, U_R)(x, \Delta t), \tag{4.44}$$

and corresponds to the integration over the domain $[-M, M] \cdot [0, \Delta t]$ of the linearized conservation equation 4.37, and we can conclude that $F^R_{1/2} - F^L_{1/2} = 0$.

Let us consider now the integration over the domain $[-M, 0] \cdot [0, \Delta t]$ of the linearized equations, it comes:

$$\int_{-M}^{0} LRP(U_L, U_R)(x, \Delta t)dt = \Delta t \left(\tilde{A}U_L - \tilde{A}[LRP(U_L, U_R)(0)]\right) - MU_L. \tag{4.45}$$

Using the expression of $[LRP(U_L, U_R)(0)]$, we have:

$$\int_{-M}^{0} LRP(U_L, U_R)(x, \Delta t)dt = -\Delta t \sum_{\lambda_l \leq 0} \alpha_l \lambda_l R_l - MU_L \tag{4.46}$$

The first term is then expressed by using Eq. 4.42 and thus, we obtain:

$$\Delta t F_L - MU_L - \Delta t F_{1/2}^L = -\Delta t \sum_{\lambda_l \leq 0} \alpha_l \lambda_l R_l - MU_L \tag{4.47}$$

which finally gives the expression of the Roe's flux:

$$F_{1/2} = F_L + \sum_{\lambda_l \leq 0} \alpha_l R_l = F_R - \sum_{\lambda_l \geq 0} \alpha_l \lambda_l R_l \tag{4.48}$$

or:

$$F_{1/2} = \frac{1}{2}(F_L + F_R) - \frac{1}{2}\sum_{i=1}^{3} \alpha_l |\lambda_l| R_l. \tag{4.49}$$

The first term corresponds to a second order centered flux and the second term is an amount of upwinding.

4.4.2 Entropy correction

What is the problem

The goal of this section is to introduce the most important drawback of the Roe's scheme, namely:

The solution may not respect the second thermodynamics principle.

First, let's consider the model problem defined by Burgers' equation:

$$\frac{\partial u}{\partial t} + \frac{\partial f(u)}{\partial x} = 0 \text{ with } f(u) = \frac{u^2}{2}. \tag{4.50}$$

Following the Roe's scheme, let's introduce the Jacobian matrix; it corresponds simply to the derivative $f'(u) = u$ and as a consequence, the first property of the Roe's linearization looks like:

$$f(u_R) - f(u_L) = \tilde{a}(u_R - u_L) \tag{4.51}$$

which gives:

$$\tilde{a} = \begin{cases} \dfrac{f(u_R) - f(u_L)}{u_R - u_L} & if \quad u_L \neq u_R \\ f'(u) & else \end{cases} \tag{4.52}$$

For Burgers' equation, the Roe's flux is given by:

$$F_{1/2} = \begin{cases} u_R^2/2 & if \quad \tilde{a} \leq 0 \\ u_L^2/2 & if \quad \tilde{a} \geq 0 \end{cases} \text{ and } \tilde{a} = \frac{u_L + u_R}{2} \tag{4.53}$$

Let's assume the initial condition to be:

$$u(x) = \begin{cases} -1 & if \quad x \leq 0 \\ +1 & else, \end{cases} \tag{4.54}$$

which numerically produces an expansion shock. The existence of expansion shocks is a violation of the second law of thermodynamics, since it implies entropy reduction. If we observe the evolution of $\tilde{a}(x)$, we have:

$$\tilde{a}(x) = \begin{cases} -1 & if \quad x < 0 \\ 0 & if \quad x = 0 \\ +1 & if \quad x > 0 \end{cases} \tag{4.55}$$

and so the upwinding term is equal to zero at the discontinuity. For the Godunov's scheme, the numerical flux is given by using Eq. 4.34:

$$f_{1/2} = \begin{cases} 1/2 & if \quad x < 0 \\ 0 & if \quad x = 0 \\ 1/2 & if \quad x > 0 \end{cases} \tag{4.56}$$

This expression show that the function $u(x)$ will evolve during time, and so the expansion shock will disappear.

How to cure the Roe's scheme

Consider the numerical Roe's flux:

$$F_{1/2} = \frac{1}{2}(F_L + F_R) - \frac{1}{2}\sum_{i=1}^{3} \alpha_l |\lambda_l| R_l, \tag{4.57}$$

one can observe that the upwinding term is zero if one of the eigenvalues is zero, and Harten proposed to replace the absolute value by a special function called the Harten-function defined by:

$$\Psi(\lambda) = \begin{cases} \frac{1}{2}\left(\frac{\lambda^2 + \delta^2}{\delta}\right) & if \quad |\lambda| < \delta \\ |\lambda| & else, \end{cases} \tag{4.58}$$

and presented in Fig. 4.4. δ is called the Harten's parameter, and is chosen by the user. Many formulations exist for this parameter:

- δ could be constant and chosen classically between 0.1 and 0.25 or,
- δ could depend on the spectral radius $\delta = \delta_1(|u|+c)$ and δ_1 is an user-specified parameter.

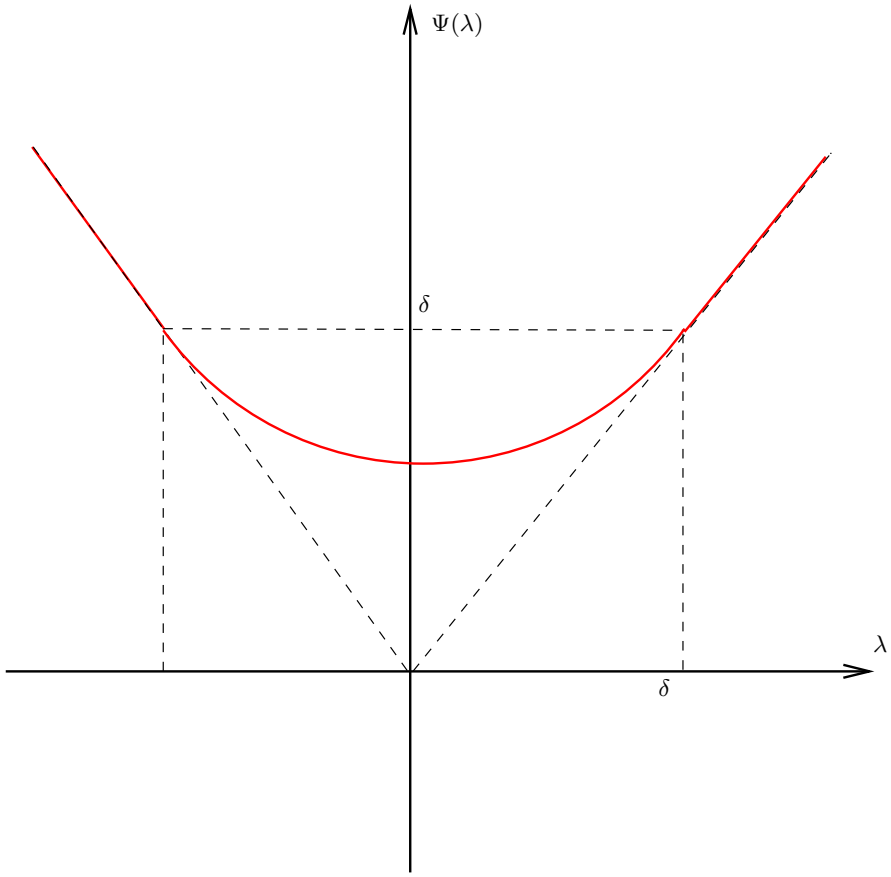

Figure 4.4: Representation of the Harten's function.

4.5 Second order schemes

The Steger-Warming's or Roe's schemes are simple to implement and have good properties, but their accuracy isn't sufficient for most of practical applications. This is due to their low level of precision (order 1). Thus, it is mandatory to introduce second order accuracy in these schemes, but the modifications to increase accuracy must be carefully done otherwise, oscillations could appear near discontinuities such as shock waves or contact discontinuity.

In the present section, we introduce a second order accurate scheme, and then we introduce some important properties such as *total variation diminishing* or *maximum principle*.

4.5.1 Variable extrapolation or MUSCL approach

MUSCL means Monotone Upstream-centered Schemes for Conservation Laws and this procedure has been proposed by Van Leer in 1979 [4]. Approximating an unknown by a piecewise constant function on a mesh is equivalent to a first-order spatial discretization. The objective of the MUSCL approach is to propose a linear approximation of the solution on each cell, which corresponds to a second order space discretization. As seen in the previous sections, the finite volume discretization could be written as:

$$\widehat{U}_i^{n+1} = \widehat{U}_i^n - \frac{\Delta t}{\Delta x}(F_{i+1/2} - F_{i-1/2}). \tag{4.59}$$

If $U^L_{i+1/2}$ and $U^R_{i+1/2}$ represent respectively the left and right values at the mesh interface $i+1/2$, a first order scheme is obtained by taking simply $U^L_{i+1/2} = U_i$ and $U^R_{i+1/2} = U_{i+1}$.

As ever explained, a second order accurate scheme is obtained with the proposed numerical schemes simply by replacing the zeroth order extrapolation at the mesh interface by a linear extrapolation. There are several ways to build this first order extrapolation and as an example, two formulations are presented below:

- **Decentered formulation**(I) This case is show on Fig. 4.5.

$$U^L_{i+1/2} = U_i + \frac{1}{2}(U_i - U_{i-1}) \tag{4.60}$$

$$U^R_{i+1/2} = U_{i+1} - \frac{1}{2}(U_{i+2} - U_{i+1}) \tag{4.61}$$

- **Centered formulation**(II) This case is show on Fig. 4.6.

$$U^L_{i+1/2} = U_i + \frac{1}{2}(U_{i+1} - U_i) \tag{4.62}$$

$$U^R_{i+1/2} = U_{i+1} - \frac{1}{2}(U_{i+1} - U_i) \tag{4.63}$$

These two formulations are generally combined into a single one by introducing a weight parameter called *precision parameter* and denoted ϕ:

$$U^L_{i+1/2} = \frac{1-\phi}{2}\left(U^L_{i+1/2}\right)^{(I)} + \frac{1+\phi}{2}\left(U^L_{i+1/2}\right)^{(II)} \tag{4.64}$$

with $-1 \leq \phi \leq +1$. Some choices for ϕ lead to special schemes:

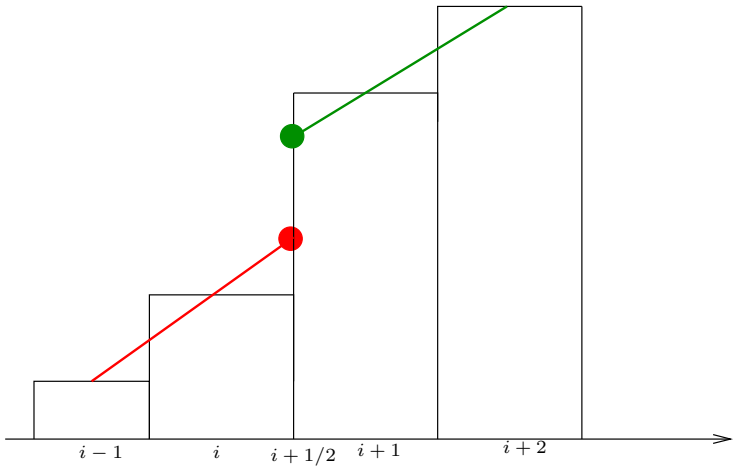

Figure 4.5: Description of the first order extrapolation for the decentered formulation.

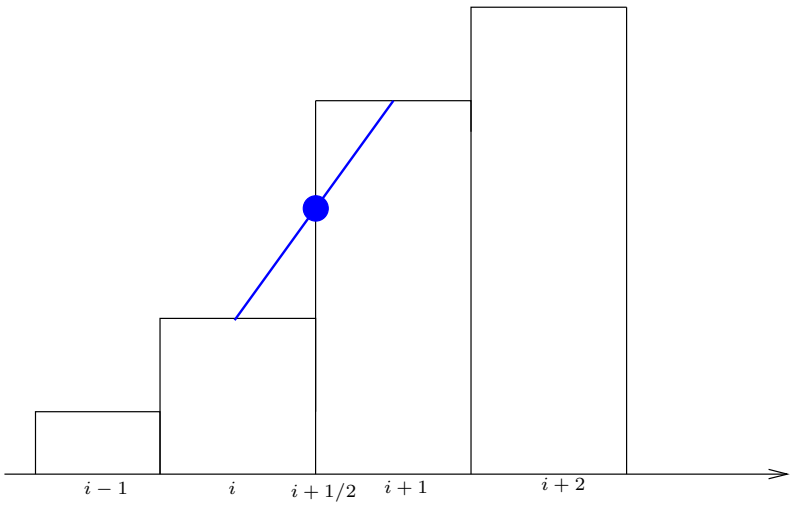

Figure 4.6: Description of the first order extrapolation for the centered formulation.

- $\phi = -1$: decentered scheme,
- $\phi = +1$: centered scheme,
- $\phi = 1/3$: third order scheme, as it could be proved by Taylor expansion arguments.

The reconstruction procedure can be applied on conservative, primitive or characteristic variables. Since the relations between these variables are not linear, the choice is not irrelevant. Our experiments for supersonic or hypersonic applications enable us to conclude that the use of characteristic variables leads to the most robust but expensive scheme, and to decrease the numerical cost, primitive variables are preferred.

This simple procedure to obtain a second order of accuracy is unfortunately not robust since oscillations could occur; as it can be seen on Fig. 4.7, which presents the evolution of the solution between t^n and t^{n+1} for a simple linear convection:

$$\frac{\partial u}{\partial t} + a\frac{\partial u}{\partial x} = 0. \tag{4.65}$$

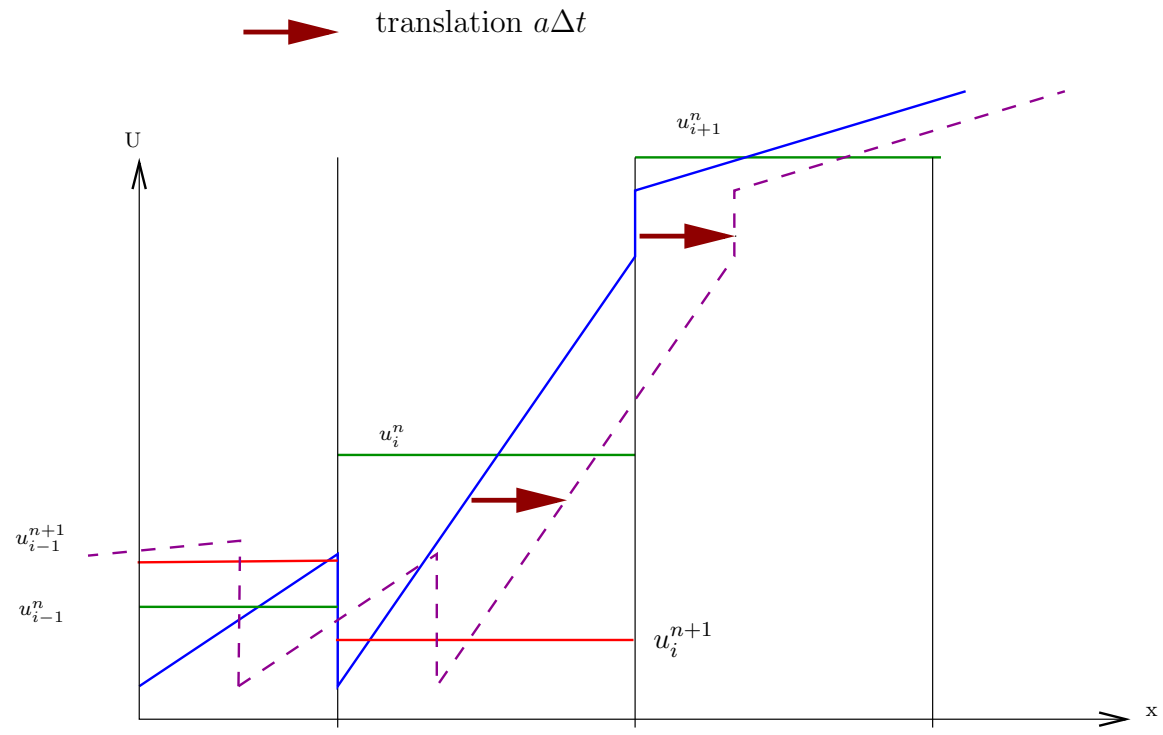

Figure 4.7: Creation of numerical oscillations for the linear convection.

At time $t = t^n$, the solution u is discretized by a piecewise function (in green) and $u_i \leq u_{i+1}$. The linear reconstruction procedure leads to the function represented in blue, which is convected at velocity a to obtain the purple function. This function is afterwards averaged, and a new constant piecewise approximation is obtained (in red) at time $t = t^{n+1}$. At this time, $u_i \geq u_{i+1}$: *an oscillation appeared*. A way of circumvent this mechanism will be proposed later by introducing slope limiters in the linear reconstruction process.

4.5.2 Flux extrapolation or non-MUSCL approach

In the last section, the state variables were extrapolated to cell interfaces and after the extrapolated values were used to compute the numerical fluxes. Since the flux function is in general nonlinear in term of state vector, another non equivalent approach could be proposed: the flux in the cells are directly extrapolated to the boundaries, defining an interface flux.

The flux extrapolation is firstly proposed for flux vector splitting and secondly for Riemann based schemes. For the positive flux, a backward extrapolation is retained, and for the negative part, a forward extrapolation is used:

$$F^+_{i+1/2} = F^+_i + \frac{1}{4}\left[(1-\phi)(F^+_i - F^+_{i-1}) + (1+\phi)(F^+_{i+1} - F^+_i)\right] \tag{4.66}$$

$$F^-_{i+1/2} = F^-_{i+1} - \frac{1}{4}\left[(1-\phi)(F^-_{i+2} - F^-_{i+1}) + (1+\phi)(F^-_{i+1} - F^-_i)\right] \tag{4.67}$$

A second order numerical flux is obtained by:

$$F^{2ord}_{i+1/2} = F^-_{1+1/2} + F^+_{i+1/2}. \tag{4.68}$$

For the Steger-Warming scheme, the computation of negative and positive parts of fluxes is clear; but for the Riemann's solver based schemes, these quantities must be determinate. If we use the Roe's scheme Eq. 4.48, the two quantities df^- and df^+ defined by:

$$df^-_{i+1/2} = F^*_{i+1/2} - F_i = \sum_{\lambda_l \le 0} \alpha_l R_l \tag{4.69}$$

$$df^+_{i+1/2} = F_{i+1} - F^*_{i+1/2} = \sum_{\lambda_l \ge 0} \alpha_l \lambda_l R_l, \tag{4.70}$$

correspond to waves which propagate respectively backward for df^- and forward for df^+. $F^*_{i+1/2}$ represents the Roe's numerical flux at interface $i+1/2$. Thus, the following relations could be assumed:

$$F^+_i - F^+_{i-1} = df^+_{i-1/2},\ F^-_{i+1} - F^-_i = df^-_{i+1/2} \text{ and } F^+_i + F^-_{i+1} = F^*_{i+1/2} \tag{4.71}$$

Finally, Eq. 4.67 becomes for the Roe's scheme:

$$F^{2ord}_{i+1/2} = F^*_{i+1/2} + \frac{1}{4}\left[(1-\phi)(F_i - F^*_{i-1/2}) + (1+\phi)(F_{i+1} - F^*_{i+1/2}\right] \tag{4.72}$$

$$+ \frac{1}{4}\left[(1-\phi)(F_{i+1} - F^*_{i+3/2}) + (1+\phi)(F_i - F^*_{i+1/2}\right] \tag{4.73}$$

4.5.3 Total Variation Diminishing (TVD)

This concept of Total Variation bounded or decreasing is based on a property of the scalar conservation law. For $\dfrac{\partial u}{\partial t} + \dfrac{\partial f(u)}{\partial x} = 0$, the total variation defined by

$$TV(u) = \int \left|\frac{\partial u}{\partial x}\right| dx \tag{4.74}$$

does not increase in time (Lax 1973). The discretized formulation of $TV(u)$ is given by:

$$TV(u) = \sum_i |u_{i+1} - u_i|. \tag{4.75}$$

A numerical scheme is said to be *Total Variation Diminishing* if $TV(u^{n+1}) < TV(u^n) \quad \forall n$.
A scheme is said to be *Monotonicity Preserving* if:

- no new local extrema in space can be created,
- the value of a local minimum (resp. maximum) is not decreasing (resp. not increasing).

One can prove that TVD schemes are Monotonicity Preserving. The principal interest of the TVD property in comparison with monotonicity lies in the fact that it is easier to impose TVD conditions to a scheme than Monotonicity Preserving.

In order to derive a TVD second order scheme, the scheme is rewritten under an increment form and let us introduce the following difference $\delta u_{i+1/2} = u_{i+1} - u_i$. The semi-discretized equation:

$$\frac{\partial u_i}{\partial t} = -\frac{1}{\Delta x}(f^*_{i+1/2} - f^*_{i-1/2}) \tag{4.76}$$

where $f^*_{i+1/2} = f^*(u_i, u_{i+1})$ is the numerical flux, is written as:

$$\frac{\partial u_i}{\partial t} = -\frac{1}{\Delta x}(C^-_{i+1/2}\delta u_{i+1/2} - C^+_{i-1/2}\delta u_{i-1/2}). \tag{4.77}$$

More precisely, we have:

$$C^-_{i+1/2}\delta u_{i+1/2} = f^*_{i+1/2} - f_i \text{ and } C^+_{i-1/2}\delta u_{i-1/2} = f_i - f^*_{i-1/2} \tag{4.78}$$

which is the contribution from waves with negative, respectively positive, wave speeds. Harten showed that the scheme given by Eq. 4.77 is TVD if and only if:

$$C^+_{i+1/2} \geq 0\ ,\ C^-_{i+1/2} \leq 0 \text{ and } 0 \leq \frac{\Delta t}{\Delta x}(C^-_{i+1/2} - C^+_{i-1/2}) \leq 1 \tag{4.79}$$

This theorem will be used to construct high order TVD scheme based on flux or variable reconstructions.

4.5.4 Flux reconstruction method: TVD scheme

To build a TVD scheme, we start for example from the expression of the second order flux (Eq. 4.73), we consider the case $\Phi = -1$, and we introduce the following flux difference ratios:

$$r^+_{i+1/2} = \frac{f_{i+2} - f^*_{i+3/2}}{f_{i+1} - f^*_{i+1/2}} \qquad r^-_{i+1/2} = \frac{f_{i-1} - f^*_{i-1/2}}{f_i - f^*_{i+1/2}} \tag{4.80}$$

with these notations, a scalar evolution equation becomes:

$$\begin{aligned} \frac{\partial u_i}{\partial t} \quad &+ \quad \frac{1}{\Delta x}\left[1 + \frac{1}{2}\Psi(r^+_{i-1/2}) - \frac{1}{2}\frac{\Psi(r^+_{i-3/2})}{r^+_{i-3/2}}\right](f_i - f^*_{i-1/2}) \\ &+ \quad \frac{1}{\Delta x}\left[1 + \frac{1}{2}\Psi(r^-_{i+1/2}) - \frac{1}{2}\frac{\Psi(r^-_{i+3/2})}{r^-_{i+3/2}}\right](f^*_{i+1/2} - f_i) \end{aligned} \tag{4.81}$$

By using the first two TVD conditions Eq. 4.79, we obtain:

$$1 + \frac{1}{2}\Psi(r^+_{i-1/2}) - \frac{1}{2}\frac{\Psi(r^+_{i-3/2})}{r^+_{i-3/2}} \geq 0 \tag{4.82}$$

$$1 + \frac{1}{2}\Psi(r^-_{i+1/2}) - \frac{1}{2}\frac{\Psi(r^-_{i+3/2})}{r^-_{i+3/2}} \geq 0 \tag{4.83}$$

These two relations are equivalent to:

$$\frac{\Psi(r)}{r} - \Psi(s) \leq 2 \quad \forall r, s \tag{4.84}$$

and thus

$$0 \leq \Psi(r) \leq \min(2r, 2) \tag{4.85}$$

Two other limits could be obtain by studying linear convection equation with Lax-Wendroff or Beam-Warming[3] schemes and lead to the TVD region shown in Fig. 4.8.

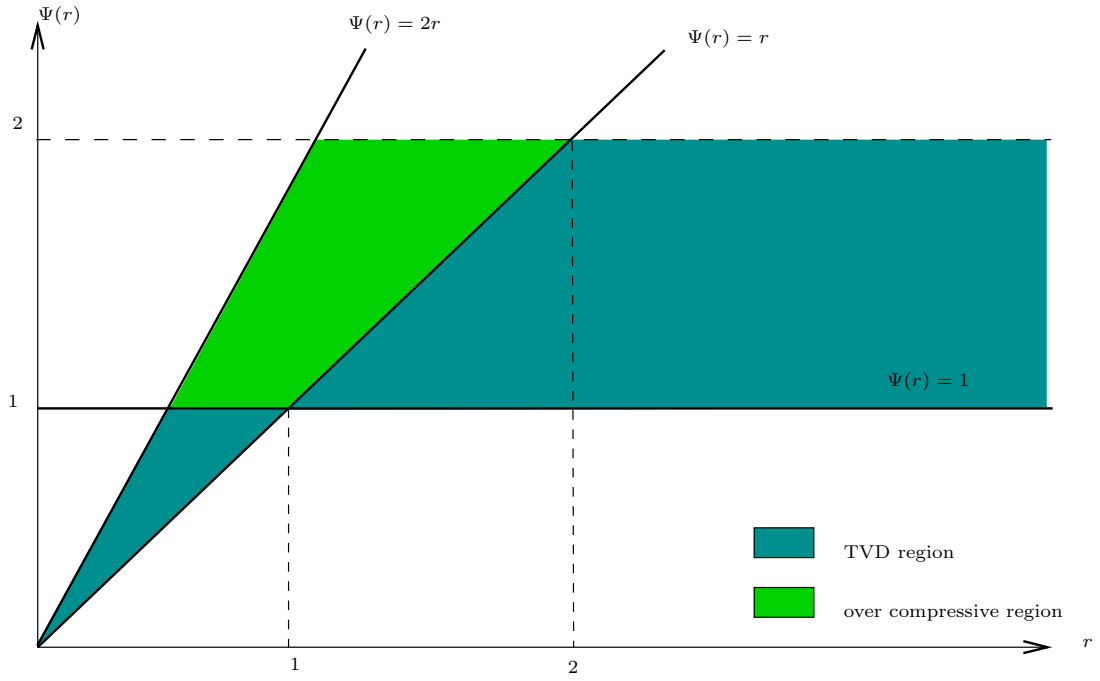

Figure 4.8: Definition of the TVD region.

For example, Sweby [8] showed that for a limiter whose graph lies in the so-called "over compressive region", the corresponding scheme transforms a sinusoidal wave into a square wave.

The third condition Eq. 4.79 corresponds to a CFL condition and consists in a limit of time step for robustness.

[3]These schemes are out of purpose of this lesson but the reader is encouraged to learn about these schemes by looking for papers on the web.

4.5.5 Variable reconstruction method: TVD scheme

Let's begin by a definition: *A scheme*

$$u_i^{n+1} = H(u_{i-r+1}^n, ..., u_{i+s}^n) \tag{4.86}$$

with r and s two non negative integers, is said monotone if $\frac{\partial H}{\partial u_j^n} \geq 0 \; \forall j$, which is equivalent to say that H is a non decreasing function of each of its arguments.

Remark 4.5.1. *Any Riemann's solver is a monotone scheme.*

The following theorem will give the basis used to build variable-reconstruction-based TVD high order schemes:

Theorem 4.5.2. *If the extrapolated values $u_{i+1/2}^L, u_{i+1/2}^R$ satisfy:*

$$\begin{cases} \min(u_{i-1}, u_i) & \leq u^L \leq & \max(u_{i-1}, u_i) \; \forall i \\ \min(u_{i+1}, u_i) & \leq u^R \leq & \max(u_{i+1}, u_i) \; \forall i \end{cases} \tag{4.87}$$

then any monotone scheme of the form:

$$v_i^{n+1} = \sum_{k=-1}^{1} b_k v_{i+k}^n \tag{4.88}$$

applied to u^L and u^R is TVD.

The monotone property is the discrete version of the following property of the exact solution of conservation law:

Lemma 4.5.3. *If two initial functions $u_0(x)$ and $v_0(x)$ satisfy $v_0(x) \geq u_0(x) \, \forall x$, then their corresponding solutions $v(x,t)$ and $u(x,t)$ satisfy $v(x,t) \geq u(x,t) \; \forall t > 0$*

One can prove that all Riemann solvers are monotone schemes and finally, building a TVD scheme based on a monotone scheme and a variable reconstruction technique needs simply to verify the two inequalities 4.87.

The limited version of the variable reconstruction procedure given by Eq. 4.89 is:

$$u_{i+1/2}^L = u_i + \frac{1}{4}\left[(1-\phi)\text{minmod}(r, b) + (1+\phi)\text{minmod}(1, br)\right](u_i - u_{i-1}) \tag{4.89}$$

and

$$r = \frac{(u_{i+1} - u_i)}{(u_i - u_{i-1})}.$$

One can prove that the following reconstruction procedure respect the inequalities 4.87 if:

$$1 \leq b \leq \frac{3-\phi}{1-\phi} \tag{4.90}$$

b is called the compression parameter since with larger values of b, the limiting procedure is less efficient and the scheme becomes too compressive.

4.6 Extension to 2-D Euler flows

All methods seen in previous sections are devoted to one dimensional conservation law, and we show now how these previous schemes could be used to discretized two- (or multi-) dimensional conservation law.

Consider the following two dimensional Euler equations:

$$\frac{\partial \widehat{U}}{\partial t} + \frac{\partial F(U)}{\partial x} + \frac{\partial G(U)}{\partial y} = 0. \tag{4.91}$$

The discretization of these equations is based on a Finite-Volume approach. In the future, the grid is assumed to be a Cartesian mesh with the mesh lines aligned with the coordinates directions x and y. An explicit finite volume scheme reads:

$$\frac{\partial \widehat{U}}{\partial t} + \frac{1}{\Delta x}\left(F_{i+1/2,j} - F_{i-1/2,j}\right) + \frac{1}{\Delta y}\left(G_{i,j+1/2} - G_{i,j-1/2}\right) = 0 \tag{4.92}$$

The problem consists now on finding an expression for the numerical interface fluxes and this will be done by using independently for each interface a one dimensional scheme: this procedure is called *dimensional splitting*. This approximation is made in all finite volume solvers, because it is nearly impossible to solve a two dimensional Riemann problem.

Another question comes from the fact that the flux function F contains a supplementary component relative to the transversal velocity:

$$F(U) = (\rho u, \rho u^2 + p, \underbrace{\rho v}_{\text{transversal term}}, \rho u H)^T \tag{4.93}$$

One can easy show that the Jacobian matrix $A = \frac{\partial F}{\partial U}$ has the latest three eigenvalues (the ones in the 1D approximation) plus one eigenvalue equal to u for the y-component of the velocity. In other words, the characteristic wave associated to this new component is a contact discontinuity (or a shear wave) and the Riemann's problem solution consists finally in a four waves system: the three waves associated with $u + c$, $u - c$ and u and a supplementary shear wave associated with u.

The last question concerns what happens when the mesh is not Cartesian, and the cell (in 2D) is a quadrilateral finite volume (we limit our course to quadrangle-based meshes which are considered structured). The two dimensional conservation equation is discretized by a finite volumes methods as:

$$V_{i,j}\frac{\partial \widehat{U}}{\partial t} + \left(\widehat{F}\right)_{i+\frac{1}{2},j} - \left(\widehat{F}\right)_{i-\frac{1}{2},j} + \left(\widehat{G}\right)_{i,j+\frac{1}{2}} - \left(\widehat{G}\right)_{i,j-\frac{1}{2}} = 0, \tag{4.94}$$

The classical notations are adopted (Fig. 4.9). $V_{i,j}$ is the volume of the cell indexed by (i, j).

$$\left(\widehat{F}\right)_{i+\frac{1}{2},j} = \begin{bmatrix} F \\ G \end{bmatrix} \cdot \vec{S}_{i+\frac{1}{2},j}, \tag{4.95}$$

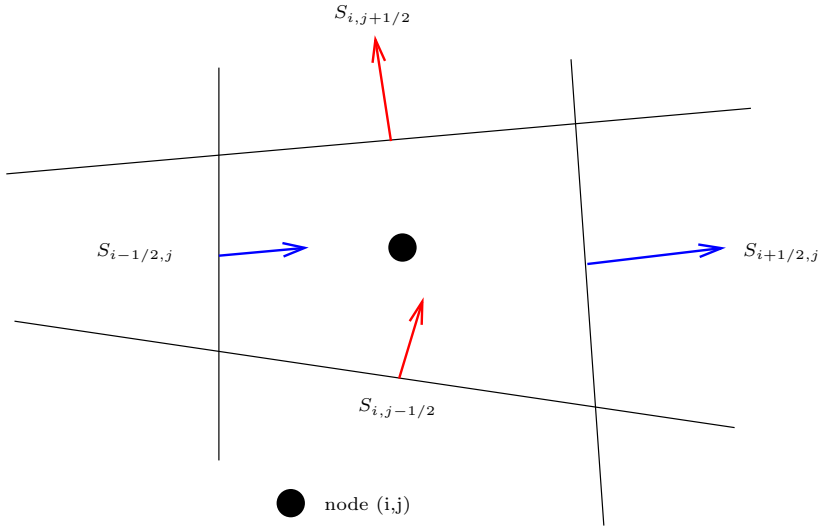

Figure 4.9: Representation of the volume and normal vectors for the Finite Volume integration.

where F and G are the convection Cartesian fluxes in direction x and y, and $\vec{S}$ is the surface vector:

$$\vec{S}_{i+\frac{1}{2},j} = \begin{bmatrix} s_1 \\ s_2 \end{bmatrix} et\, \vec{S}_{i,j+\frac{1}{2}} = \begin{bmatrix} s_3 \\ s_4 \end{bmatrix}, \tag{4.96}$$

thus, we have:

$$\left(\widehat{F}\right)_{i+\frac{1}{2},j} = s_1 (F)_{i+\frac{1}{2},j} + s_2 (G)_{i,j+\frac{1}{2}}. \tag{4.97}$$

In the two dimensional context, the cell is also defined by four straight segments. We consider only two-order accurate schemes (associated with a metric computed at a second order of accuracy), and effects of cells curvature would not be taken into account[4].

If n_s denotes the unit vector normal to the face indexed by s, we have $n_s = (cos(\theta_s), sin(\theta_s))$. The total flux balance in Eq. 4.94 could be written as:

$$\sum_{s=1}^{4} \ell_s \left[cos(\theta_s) F(U) + sin(\theta_s) G(U)\right] \tag{4.98}$$

where ℓ_s is the length of the line indexed by s. If we use the *rotational invariance of the Euler equations*, we have:

$$cos(\theta_s) F(U) + sin(\theta_s) G(U) = T_s^{-1} F(T_s U) \tag{4.99}$$

where T_s is the rotation matrix associated with the θ_s and T_s^{-1} is its inverse, namely:

$$T(\theta) = \begin{bmatrix} 1 & 0 & 0 & 0 \\ 0 & cos(\theta) & sin(\theta) & 0 \\ 0 & -sin(\theta) & cos(\theta) & 0 \\ 0 & 0 & 0 & 1 \end{bmatrix} \tag{4.100}$$

[4]For most of the novel high order convection schemes, curvature effects must be taken into account since the precision of these schemes depends also on the precision of the discretization and therefore on the metric considered in the computations.

Now if we consider the rotated state vector $T_s U$, its second component corresponds to the velocity aligned with the normal vector to the face n_s, and the third component is the tangential velocity. Thus, we have a strictly one-dimensional problem for this rotated state vector, and we can use the flux formulations presented earlier.

4.7 Time integration methods

In most of the previous sections, the time derivative was left in its continuous form and was not discretized. To solve an Ordinary Differential Equation, many numerical techniques are available, for example Runge Kutta, Predictor-Corrector, or the simplest one called Backward Euler, which is first order in time. To solve the ODE $\frac{du}{dt} = f(u,t)$, the Backward Euler approach reads:

$$\frac{u(t+dt)-u(t)}{dt} = f(u,t) \text{ or } u^{n+1} = u^n + f(u^n, t^n)dt\,. \tag{4.101}$$

With a Taylor expansion in time, one can prove that this scheme is first order accurate, and by increasing the degree of the polynomial approximation in Eq. 4.101, one can build a more accurate discretization of the so called BDF schemes family. The scheme given by Eq. 4.101 is said *explicit* since when the state vector is known at time n, we can compute directly the state vector at time $n+1$.

When using the explicit time integration Eq. 4.101, the associated time step must be very small for robustness reason: the Courant Friedich Lewy coefficient which links time and space steps must be lower than 1 and in practice is of order 0.5. To use larger time step, an *implicit* time integration scheme is needed:

$$u^{n+1} = u^n + f(u^{n+1}, t^{n+1})dt. \tag{4.102}$$

In this case, the state vector values at time $n+1$ is obtained by solving the nonlinear equation Eq. 4.102, which reads:

$$g(x) = u^n + f(x, t^{n+1}) - x = 0. \tag{4.103}$$

Eq. 4.103 is solved with the Newton method which is an iterative approach, written as follows for a scalar equation:

$$x^{\nu+1} = x^\nu - \frac{f(x^\nu)}{f'(x^\nu)}, \tag{4.104}$$

or as follows for a nonlinear system:

$$f'(x^\nu)[x^{\nu+1} - x^\nu] = f(x^\nu). \tag{4.105}$$

There exist more sophisticated Newton methods which make use of the second order (time) derivative of f but they are not use in the context of implicit time integration method.

Actually, a step of the iterative Newton method leads to the resolution of a linear system, which dimensions are equal to the number of cells, and so could be very large. In practice, a global resolution is prohibited for industrial applications. To simplify the resolution, we must

take into account the graph of the f' matrix (the Jacobian of f): this matrix has many element equal to zero.

In the following, we denote $f(i,j)$ the flux balance of Eq. 4.92. By using discretization scheme, this flux balance depends on many points:

$$f(i,j) = fonct\left[U(i-l,j-k), U(i-l+1,j-k), ..., U(i,j), ..., U(i+l,j+k)\right] \quad (4.106)$$

For a first order scheme, $k = l = 1$ (three points scheme) and $k = l = 2$ for a second order ones. Using this notation, the Jacobian f' of the flux balance in Eq. 4.105 is calculated by taking the partial derivative of f (Eq.4.106) by each state vector such as $U(i-l+l_1, j-k+k_1)$ for $(l_1,k_1) \in [0,2l] * [0,2k]$. Finally, the iteration ν of the Newton's procedure could be written as:

$$\begin{aligned}\left(\frac{V_{i,j}}{\Delta t}\right)\Delta U_{i,j} \quad &+ \quad \left(\frac{\partial f(i,j)}{\partial U_{i-l,j-k}}\right)\Delta U_{i-l,j-k} + \left(\frac{\partial f(i,j)}{\partial U_{i-l+1,j-k}}\right)\Delta U_{i-l+1,j-k} + ... \\ &+ \quad \left(\frac{\partial f(i,j)}{\partial U_{i,j}}\right)\Delta U_{i,j} + \left(\frac{\partial f(i,j)}{\partial U_{i+l,j+k}}\right)\Delta U_{i+l,j+k} = -f(i,j) \end{aligned} \quad (4.107)$$

where:

$$\Delta U_{i,j} = \left(U_{i,j}^{\nu+1} - U_{i,j}^{\nu}\right) \quad (4.108)$$

and we recall that the notation $f(i,j)$ **correspond to the flux balance through the cell indexed by** (i,j) **calculated with the state vector** U^{ν}.

We have now to compute all terms of the Jacobian matrix, or more exactly an approximation of them. To give an example, we consider the case when the Roe's scheme is used. Firstly, the Eq. 4.49 could be written in a more compact form:

$$F_{i+1/2,j} = \frac{1}{2}\left(F_{i+1,j} + F_{i,j}\right) - \frac{1}{2}|A|_{i+1/2,j}(U_{i+1,j} - U_{i,j}) \quad (4.109)$$

where:

$$|A| = R\Psi_H|\Lambda|R^{-1} \quad (4.110)$$

Ψ_H is the Harten function and R (resp. R^{-1}) are the matrix of the right (resp. left) eigenvectors. For witting this final form, we consider the most general case of a two-dimensionnal non Cartesian grid, and so the finite volume discretization is given by Eq. 4.94. We recall that:

$$\left(\widehat{F}\right)_{i+1/2,j} = F_{i+1/2,j}\vec{S}_{i+1/2,j}\cdot\vec{x} + G_{i,j+1/2}\vec{S}_{i+1/2,j}\cdot\vec{y}, \quad (4.111)$$

with $\vec{x} = (1,0)$ and $\vec{y} = (0,1)$. For the Jacobian matrix, we have:

$$\frac{\partial\left(\widehat{F}\right)_{i+1/2,j}}{\partial U} = \frac{\partial F_{i+1/2,j}}{\partial U}\vec{S}_{i+1/2,j}\cdot\vec{x} + \frac{\partial G_{i,j+1/2}}{\partial U}\vec{S}_{i+1/2,j}\cdot\vec{y} \quad (4.112)$$

We adopt the following notations:

$$A(U_{i,j}, S_{i+1/2,j}) = \frac{\partial F}{\partial U}(U_{i,j})\vec{S}_{i+1/2,j}\cdot\vec{x} + \frac{\partial G}{\partial U}\vec{S}_{i+1/2,j}\cdot\vec{y} \quad (4.113)$$

Remember that Roe replaced the Jacobian matrix by a constant matrix which does not depend on the state vector and therefore:

$$\frac{\partial \widehat{F}_{i+1/2,j}}{\partial U_{i,j}} = \frac{1}{2}A(U_{i,j}, S_{i+1/2,j}) + \frac{1}{2}|A|_{i+1/2,j} \tag{4.114}$$

and

$$\frac{\partial F_{i+1/2,j}}{\partial U_{i+1,j}} = \frac{1}{2}A(U_{i+1,j}, S_{i+1/2,j}) - \frac{1}{2}|A|_{i+1/2,j} \tag{4.115}$$

Finally, the implicit linear system could be given for the node (i, j) by:

$$(\Lambda_0)_{i,j}\Delta U_{i,j}+(\Lambda_1)_{i,j}\Delta U_{i+1,j}+(\Lambda_2)_{i,j}\Delta U_{i-1,j}+(\Lambda_3)_{i,j}\Delta U_{i,j+1}+(\Lambda_4)_{i,j}\Delta U_{i,j-1} = -f_{i,j} \tag{4.116}$$

with:

$$(\Lambda_0)_{i,j} = \frac{V_{i,j}}{\Delta t} + \frac{1}{2}\left(A(U_{i,j}, S_{i+1/2,j}) + \frac{1}{2}|A|_{i+1/2,j}\right) \tag{4.117}$$

$$- \frac{1}{2}\left(A(U_{i,j}, S_{i-1/2,j}) - \frac{1}{2}|A|_{i-1/2,j}\right) \tag{4.118}$$

$$+ \frac{1}{2}\left(A(U_{i,j}, S_{i,j+1/2}) + \frac{1}{2}|A|_{i,j+1/2}\right) \tag{4.119}$$

$$- \frac{1}{2}\left(A(U_{i,j}, S_{i,j-1/2}) - \frac{1}{2}|A|_{i,j-1/2}\right) \tag{4.120}$$

and:

$$(\Lambda_1)_{i,j} = \frac{1}{2}A(U_{i+1,j}, S_{i+1/2,j}) - \frac{1}{2}|A|_{i+1/2,j} \tag{4.121}$$

$$(\Lambda_2)_{i,j} = \frac{1}{2}A(U_{i-1,j}, S_{i-1/2,j}) + \frac{1}{2}|A|_{i-1/2,j} \tag{4.122}$$

$$(\Lambda_3)_{i,j} = \frac{1}{2}A(U_{i,j+1}, S_{i,j+1/2}) - \frac{1}{2}|A|_{i,j+1/2} \tag{4.123}$$

$$(\Lambda_4)_{i,j} = \frac{1}{2}A(U_{i,j-1}, S_{i,j-1/2}) + \frac{1}{2}|A|_{i,j-1/2} \tag{4.124}$$

Note that $(\Lambda_l)_{i,j}$ is a matrix of dimension 4×4.

To solve this block pentadiagonal system, several methods are available and we adopt here the so-called DDADI method (Diagonally Dominant Alternate Direction Iterative method). This method is based on an approximate factorization of the previous linear system. If X is the vector whose components are the $\Delta U_{i,j}$, the previous system could be written as:

$$(D + N + M)X = Rhs, \tag{4.125}$$

where D is the block diagonal matrix with $(\Lambda_0)_{i,j}$ on the diagonal, N is a two off-diagonal matrix with $(\Lambda_1)_{i,j}$ on the first upper diagonal and $(\Lambda_2)_{i,j}$ on the first lower diagonal. N contains only influence in i direction and M in j direction. The factorization could be written as:

$$(D + N)D^{-1}(D + M)X = Rhs, \tag{4.126}$$

which means in fact that the resolution needs the inversion of two tridiagonal systems solved efficiently by the Thomas' algorithm. In practice, for pseudo-unstationary problems, just one Newton iteration is performed and for unstationary problems, it depends on the ratio between the numerical time steps and the characteristic time for the evolution of the physical problem. For example, if the physical problem is driven by low frequency phenomenon, the numerical time step would be very small in regard to this physics and one Newton iteration will be enough. For LES computations, where the physical time steps are very small, the Newton procedure must be continued until convergence.

Chapter 5

Conclusion

This course is designed as an introduction to CFD with respect to the choice of the scheme to discretize convection. After the presentation of all necessary notations / notions for numerical schemes, centered schemes have been quickly introduced. Our aim was to go further in the development and to treat with details the upwind convection schemes. This choice is motivated by physics rather than by mathematical arguments.

Finally, the last chapter concerns the discretization with classical upwind schemes and a link is done with the multi-dimension Riemann problem and with the time integration procedure. This was to understand that the time integration efficiency (in implicit in particular) is driven by the numerical stencil used for the spatial approximation. Such an approach is used also by the third order scheme implemented in AVBP for which the Taylor approximation treats time and spatial derivatives at the same time (TTGC scheme). Of course, for sake of clarity, the TTGC scheme has not been introduced in this document.

In the past, the Riemann solver-based schemes were chosen for their robustness property for industrial application. Extended to second order accuracy, they are the most used schemes in CFD. Nowadays, with the increase of computer efficiency, more accurate computations are available even on complex geometries and complex turbulent interactions or noise generation could be reach. To deal with these new applications, numerical schemes must be non dissipative (more precisely do not not introduce more dissipation than the physical ones) and not dispersive to preserve the waves propagation. The main drawback of the Riemann solver based scheme are the poor spectral property: they are too dispersive, and new numerical tools have been develop without the use of Riemann solvers.

However, many authors such as Drikakis or Adams, showed recently that the dissipative behavior of the fine turbulent structures could be modeled with Riemann solver-based schemes and these schemes coupled with new high order extension formulations can efficiently be used for LES simulations. As an example, the dispersive nature of these schemes has been overcome with recent approaches such as Discontinuous Galerkin or Spectral differences. The high order reconstruction improves greatly the spectral properties of the underlying Riemann solver and can in fact be used for acoustic computations. Finally, Riemann-based solvers remain one of the most important discretization tools for CFD.

Bibliography

[1] B. Després. *Lois de Conservations Eulériennes, Lagrangiennes et Méthodes Numériques*. Springer Ed., Mathématiques et Applications 68, 2010.

[2] A. Jameson, W. Schmidt, and E. Turkel. Numerical solution of the Euler equations by finite volume methods using Runge-Kutta time-stepping schemes. In *14th Fluid and Plasma Dynamic Conference June 23-25, 1981, Palo Alto, California*, 1981. AIAA paper 1981-1259.

[3] A. G. Kravchenko and P. Moin. On the effect of numerical erros in large eddy simulations of turbulent flows. *Journal of Computaitona Physics*, 131:310–322, 1997.

[4] B. Van Leer. Towards the ultimate conservative difference scheme. v. A second-order sequel to Godunov's method. *Journal of Computational Physics*, 32:101–136, 1979.

[5] P.L. Roe. Approximate Riemann solvers, parameter vectors and difference schemes. *Journal of Computational Physics*, 43:357–372, 1981.

[6] J. L. Steger. Coefficient matrices for implicit finite difference solution of the inviscid fluid conservation law equations. *Computer Methods in Applied Mechanics and Engineering*, 13(2):175–188, 1978.

[7] J. L. Steger and R. F. Warming. Flux vector splitting of the inviscid gas-dynamic equation with applications to finite difference method. *Journal of Fluid Dynamics*, 40:263–293, 1981.

[8] P. K. Sweby. High resolution schemes using flux limiters for hyperbolic conservation laws. *SIAM Journal of Numerical Analysis*, 21:995–1011, 1984.